Received: 6 December 2022 | Revised: 16 April 2023 | Accepted: 21 April 2023

DOI: 10.1111/cas.15840

ORIGINAL ARTICLE

Cancer Science WILEY

Novel and efficient method for culturing patient-derived gastric cancer stem cells

Tomonori Morimoto[1,2] | Yukitoshi Takemura[3] | Takemitsu Miura[4] | Takehito Yamamoto[5] | Fumihiko Kakizaki[1] | Hideo An[1,2] | Hisatsugu Maekawa[2,3] | Tadayoshi Yamaura[1,2] | Kenji Kawada[2] | Yoshiharu Sakai[2] | Yoshiaki Yuba[5] | Hiroaki Terajima[5] | Kazutaka Obama[2] | Makoto Mark Taketo[1,5] | Hiroyuki Miyoshi[1]

[1]Colon Cancer Project, Kyoto University Hospital-iACT, Graduate School of Medicine, Kyoto University, Kyoto, Japan

[2]Department of Surgery, Graduate School of Medicine, Kyoto University, Kyoto, Japan

[3]Department of Personalized Cancer Medicine, Graduate School of Medicine, Kyoto University, Kyoto, Japan

[4]SCREEN Holdings Co., Ltd., Kyoto, Japan

[5]Medical Research Institute Kitano Hospital, Osaka, Japan

Correspondence
Hiroyuki Miyoshi, Colon Cancer Project, Kyoto University Hospital-iACT, Graduate School of Medicine, Kyoto University (Main Campus), Yoshida-Honmachi (Res. Bldg 16, Rm 107), Sakyo-ku, Kyoto 606-8501, Japan.
Email: hmiyoshi@mfour.med.kyoyo-u.ac.jp

Present address
Tadayoshi Yamaura, National Hospital Organization, Himeji Medical Center, Himeji, Japan
Kenji Kawada, Kurashiki Central Hospital, Kurashiki, Japan
Yoshiharu Sakai, Japanese Red Cross Osaka Hospital, Osaka, Japan

Funding information
Institute for Advancement of Clinical and Translational Science, Kyoto University Hospital; Japan Agency for Medical Research and Development, Grant/Award Number: ck0106195h; Japan Science and Technology Agency, Grant/Award Number: ST261001TT; Japan Society for the Promotion of Science, Grant/Award Number: JP18H02639, JP21K06948 and JP22K07187; Kyo Diagnostics K.K.; Kyoto University Office of Society-Academia Collaboration for Innovation; SCREEN Holdings Co., Ltd.

Abstract

Experimental techniques for patient-derived cancer stem-cell organoids/spheroids can be powerful diagnostic tools for personalized chemotherapy. However, establishing their cultures from gastric cancer remains challenging due to low culture efficiency and cumbersome methods. To propagate gastric cancer cells as highly proliferative stem-cell spheroids in vitro, we initially used a similar method to that for colorectal cancer stem cells, which, unfortunately, resulted in a low success rate (25%, 18 of 71 cases). We scrutinized the protocol and found that the unsuccessful cases were largely caused by the paucity of cancer stem cells in the sampled tissues as well as insufficient culture media. To overcome these obstacles, we extensively revised our sample collection protocol and culture conditions. We then investigated the following second cohort and, consequently, achieved a significantly higher success rate (88%, 29 of 33 cases). One of the key improvements included new sampling procedures

Abbreviations: CI, confidence interval; CM, conditioned medium; CRC, colorectal cancer; EGF, epidermal growth factor; GC, gastric cancer; GEI, growth effect index; NGE-SC, normal gastric epithelial stem cell; PD, patient-derived; RNA-seq, RNA sequencing; SC, stem cell; WHO, World Health Organization.

for tumor tissues from wider and deeper areas of gastric cancer specimens, which allowed securing cancer stem cells more reproducibly. Additionally, we embedded tumor epithelial pieces separately in both Matrigel and collagen type-I as their preference to the extracellular matrix was different depending on the tumors. We also added a low concentration of Wnt ligands to the culture, which helped the growth of occasional Wnt-responsive gastric cancer stem-cell spheroids without allowing proliferation of the normal gastric epithelial stem cells. This newly improved spheroid culture method may facilitate further studies, including personalized drug-sensitivity tests prior to drug therapy.

KEYWORDS
extracellular matrix, gastric cancer, spheroid, stem cell, Wnt

1 | INTRODUCTION

Gastric cancer (GC) is the fifth most common cancer in the world and fourth leading cause of cancer death even with significant improvements in surgical techniques and chemotherapy.[1,2] Histopathologically, GC comprises intestinal and diffuse types according to Lauren's classification,[3] which are further subdivided according to the World Health Organization (WHO) classification.[4] Recently, The Cancer Genome Atlas[5] and Asian Cancer Research Group[6] proposed molecular classifications based on the gene expression profiles. However, these classifications are of limited help in determining the most efficacious treatments, necessitating a personalized strategy. Currently, a few diagnostic markers are available to select suitable GC patients for treatment with therapeutic antibodies, such as those against HER2[7] and PD-1/PD-L1.[8,9] Since only a small proportion of patients can benefit from each therapy, more diagnostic tools are needed to stratify patients for current and upcoming therapies so that specific GC subpopulations can be effectively targeted.

Among possibly promising strategies for personalized cancer treatments, a more direct approach is to test the drug sensitivity of patient-derived (PD) cancer stem cells (SCs) in vitro and/or in mouse xenografts. Recently, testing PD cancer stem-cell organoids have become feasible as a clinically relevant tool for investigating personalized therapeutics,[10,11] as exemplified by those derived from colorectal cancer (CRC).[12] When it comes to GC, however, the success rates for establishing GC-SC lines are substantially lower than those for CRC-SC, with cumbersome culture methods owing to various supplementary factors and selection drugs needed for specific subtypes of GC.[13–20]

Recently, we have reported an efficient method for culturing PD–CRC-SCs[21] based on the method for normal intestinal epithelial stem cells.[22–24] These cells embedded in Matrigel form nearly spherical structures, termed spheroids, that are comprised of nearly all mitotic stem/progenitor cells, in contrast to intestinal organoids with the budding structures that comprise mixed populations of mitotic and post-mitotic cells.[25] In the present study, we have modified this conventional culture method for propagating PD–GC-SC spheroids so that we can apply it for personalized clinical diagnosis and treatment.

2 | MATERIALS AND METHODS

2.1 | Human samples

Tumor samples were collected from GC patients who underwent primary resections at the Kyoto University Hospital (KUHP, Kyoto, Japan) and Medical Research Institute Kitano Hospital (Osaka, Japan) from January 2016 to November 2022. Their diagnosis was confirmed through histopathological examinations by board-certified diagnostic pathologists.

2.2 | L-WRN conditioned medium

The L-WRN cells expressing mouse Wnt3a, R-spondin 3, and Noggin were obtained from Dr. Thaddeus S. Stappenbeck (Cleveland Clinic). Conditioned medium (CM) from L-WRN cells was prepared according to a previous protocol.[22] Quality control testing of L-WRN CM was conducted according to the validation procedures and guidelines reported previously.[26] A commercial L-WRN CM was purchased from Sigma-Aldrich.

2.3 | Spheroid culture of human gastric cancer and normal gastric epithelial cells

Immediately after surgical resection, the excised stomach by operation was opened longitudinally, wrapped in gauze moistened with saline to prevent drying, and kept at room temperature. Sample specimens were collected within 1 h after the resection operation.

From each stomach, one to four tumor pieces (100–1000 mm^3 each) and one to two pieces of normal mucosa (500–2000 mm^3) were collected in separate 15-mL conical tubes containing 5–10 mL ice-cold washing medium (Table S1). Sample tubes were kept on ice during transportation to the laboratory, and the isolation of epithelial cells and preparation of stem cell culture were performed within 6 h after sample collection (i.e., 7 h after the resection operation) according to a step-by-step protocol.[22] Specifically, the specimen pieces were minced in a 60-mm Petri dish, digested with 1–3 mL collagenase solution (Table S1) at 37°C for 40–60 min and dissociated by pipetting. Epithelial cell clusters were filtered through a 100-μm cell strainer (Corning), collected in a 1.5-mL tube, and resuspended in Matrigel (Corning) or collagen type-I matrix (Cellmatrix, Nitta Gelatin). The cell-matrix mixture was placed at the center of each well of the 12-well cell-culture plate (30 μL/well; TPP). After polymerization of matrix materials at 37°C, GC and normal gastric epithelial (NGE) cells were cultured with the cancer medium and eL-WRN medium (epidermal growth factor [EGF]-containing 50% L-WRN CM), respectively (Table S1). The medium was changed every other day. To passage, we collected Matrigel-embedded spheroids and treated them with 2.5 g/L trypsin solution (Nacalai Tesque) at 37°C for 2–5 min. Collagen type-I–embedded spheroids were treated with collagenase solution at 37°C for 30 min, followed by trypsinization. Spheroids were dissociated into small cell aggregates by pipetting, and they were resuspended in Matrigel or collagen type-I. Dilution (based on the volume of matrix materials) was adjusted to one to six times depending on the growth rate and spheroid density. It should be noted that too much trypsinization and pipetting caused poor cell survival when spheroids grew poorly in early passages. The spheroid culture was considered successful when spheroids were expanded to 12 wells of a 12-well cell-culture plate.

2.4 | Growth monitoring in spheroid culture using a cell imager

To monitor cell growth, we resuspended trypsinized spheroids in Matrigel or collagen type-I at a density of approximately 150 cell aggregates/μL. Subsequently, 3 μL cell-matrix mixture was distributed in each well of the 96-well cell-culture plate (TPP). After polymerization of matrix materials, cells were cultured in 100 μL of media. High-resolution cell images were obtained using a cell imager (Cell^{3}iMager duos, SCREEN) every 3–4 days (Figure S1A). The area of each spheroid in each well was outlined using image processing software (Figure S1B). The volume of each spheroid was estimated using the following formula: spheroid volume (μm^3) = $4/3 \times \{[\text{spheroid area } (\mu m^2)]^3/\pi\}^{1/2}$. The cell growth rate for each well was estimated as the proportion of total spheroid volume to that on initial measurement, and the growth effect index (GEI) was defined as the relative growth rate of an experimental group to that of its control group. At least three independent experiments were performed for each analysis.

2.5 | Mutational analysis

The exonic regions of 409 cancer-related genes in GC-SC spheroids were sequenced using the Ion AmpliSeq Comprehensive Cancer Panel (Thermo Fisher), and the sequence alignment to the reference genome (hg19) and variant calling were performed at Macrogen Japan. We omitted the analyses of the primary tumors because we and others had shown homogeneity of driver-gene mutations in cancer and their stability during ex vivo culture.[14,27,28] Detection of cancer-specific mutations was performed as we described previously with modifications.[27] Specifically, polymorphic alleles were removed from the called variants using the VCFtools program (V.0.1.13)[29] by referring to the GEM Japan Whole Genome Aggregation (GEM-J WGA) panel (https://togovar.biosciencedbc.jp/doc/datasets/gem_j_wga) or the profiles of NGE-SC spheroids from the same patients (when available). The selected variants were annotated using the ANNOVAR program,[30] and polymorphic alleles were removed again by referring to the Human Genetic Variation Database.[31,32] Subsequently, they were filtered to select nonsynonymous, frameshift, and splicing mutations with more than 20% frequency. Variant calls that appeared in more than two lines were eliminated as false-positive except for those identified in the COSMIC database. Other erroneous mutations were eliminated by surveying their coverage tracks on the Integrative Genomics Viewer software (V.2.12.3, Broad Institute).

2.6 | Mutation detection from RNA sequencing (RNA-seq) data

To save time and cost, we took advantage of our transcriptome analysis data that we completed in most GC-SC spheroid lines. Namely, mutations in cancer-related genes were determined by deducing from the sequences of the RNA-seq data. Spheroid RNA samples were purified using the NucleoSpin RNA II kit (Takara Bio), and RNA-seq analysis was performed at Macrogen Japan. The sequence alignment to the reference genome (hg19) and variant calling were performed using the Subio Platform software (V.1.24.5853, Subio). Cancer-specific mutations in the exonic regions of expressed genes were detected with the same workflow as for the cancer panel.

Additional Materials and Methods can be found in Appendix S1.

3 | RESULTS

3.1 | Improvement of patient-derived gastric cancer stem-cell spheroid culture efficiency using a revised protocol

To culture GC-SC spheroids, we conducted two sets of experiments in which we collected tumor samples from 71 patients of the first cohort, followed by those from 33 patients of the second. To the first cohort samples, we applied our conventional method originally

developed for CRC-SC spheroids (Table 1). Namely, we cultured tumor epithelial cells in a serum-containing cancer medium (Table S1) to propagate GC-SC spheroids.[21] In contrast, NGE-SC spheroids were also established from normal mucosa of the same patients using the eL-WRN medium (Table S1) containing mouse Wnt3a, R-spondin 3, and Noggin.[21,22] The success rate for establishing GC-SC spheroids was 25% (18 of 71 cases; 95% CI, 15%–35%), whereas that for NGE-SC spheroids was 94% (67 of 71 cases; 95% CI, 89%–100%; Table 1; Table S2). To improve the low success rate, we revised our protocol in the following three points and tested its feasibility with fresh GC samples of the second patient cohort (Table 1). First and foremost, we scrutinized the sample collection maneuver from cancer tissues. One of the major reasons for our earlier failure in GC-SC spheroid establishment by our conventional method was likely the paucity of cancer stem cells in the sampled tumor pieces as estimated histopathologically in a retrospective manner (47% with 95% CI, 30%–64%; in 16 of the 34 failed cases; Figure 1A). Another minor cause was fungal contamination (9% with 95% CI, 2%–17%; in five of the 53 failed cases), particularly, of those samples from necrotic lesions that tended to accumulate fungi and/or hyphae (Figure 1B). Therefore, we collected more tumor pieces from wider and deeper areas, avoiding necrotic lesions to harvest cancer stem cells more reproducibly (Figure 1C,D). Importantly, the revised protocol reviewed by board-certified diagnostic pathologists of the collaborating hospitals did not affect pathological and molecular pathological assessment. Second, we embedded tumor epithelial pieces of each patient in both Matrigel and collagen type-I separately. This was because the different extracellular matrix (ECM) was preferred in some minority cases. Third, we added 5% L-WRN CM (containing Wnt ligands) to the cancer medium to help propagate Wnt-responsive GC-SCs, as the extent of dependence of GC-SC organoids on Wnt ligands has been variable.[13,33] Owing to these changes, we achieved a significantly higher success rate (88% with 95% CI, 77%–99%; 29 of 33 cases) as compared to that (25% with 95% CI, 15%–35%; 18 of 71 cases) with the first patient cohort (Table 1; Table S3). We failed in four of 33 cases because of heavy contamination with yeasts (two cases) or poor cell growth in early passages (two cases). Notably, five of 29 lines (17%) were established only when embedded in collagen type-I with a statistically significant difference ($p=0.008$, Fisher's exact test), whereas three lines (10%) were only in Matrigel (Figure 2A). Regarding Wnt dependency, five GC-SC lines required L-WRN CM to maintain spheroid lines (Figure 2A). Our revised method also improved the culture efficiency in terms of the time needed for spheroid culture establishment, as the median time of the second cohort (21 days) was significantly shorter than that of the first cohort (33.5 days; Figure 2B).

Typically, GC cells formed spherical aggregates in either Matrigel or collagen type-I (Figure S2A), and they were highly proliferative in the cancer medium (Figure S2B). Their structures and expression of markers such as CDX2 and MUC2 recapitulated those in the

TABLE 1 Summary of culture methods.

	Our conventional method	Our improved method	Nanki et al.[13]	Yan et al.[14]
Sampling method				
Site	Inside the tumor boundary	Both sides of the tumor boundary	NS	NS
Number of tissue pieces	1–2	3–4	NS	NS
Area (mm^2)/Depth (mm)	50–150/2–3	100–200/3–5	NS	NS
Matrix material	Matrigel	Matrigel and collagen-I, separately	Matrigel	Matrigel
Medium composition				
Growth factor	EGF, FGF2, FBS	EGF, FGF2, FBS	EGF, FGF10	EGF, FGF10, FBS (as CM)
Stem cell niche factor	–	L-WRN CM	Afamin-Wnt3a CM, RSPO1, Noggin	Wnt3a CM, RSPO1 CM, Noggin CM
Inhibitor	SB431542, Y27632	SB431542, Y27632	A83-01	A83-01, Y27632
Other supplements	B27, NECA	B27, NECA	B27, Gastrin, NAC	B27, Gastrin, NAC
Selection procedure for cancer cell enrichment	No selection	No selection	+Nutlin-3, –A83-01/+TGF-β, –EGF/–FGF10, or single-cell dissociation	Manual picking or +Nutlin-3
Success rate	25% (18/71) (95% CI, 15%–35%)	88% (29/33) (95% CI, 77%–99%)	75% (44/59)	>50%

Note: Two representative methods reported previously are also shown as references.

Abbreviations: –, no or withdrawal from the culture medium; +, addition to the culture medium; CI, confidence interval; CM, conditioned medium; EGF, epidermal growth factor; FBS, fetal bovine serum; FGF, fibroblast growth factor; NAC, *N*-Acetyl-L-cysteine; NECA, 5′-*N*-ethylcarboxamine adenosine; NS, not specified; RSPO1, R-spondin 1; TGF-β, transforming growth factor beta.

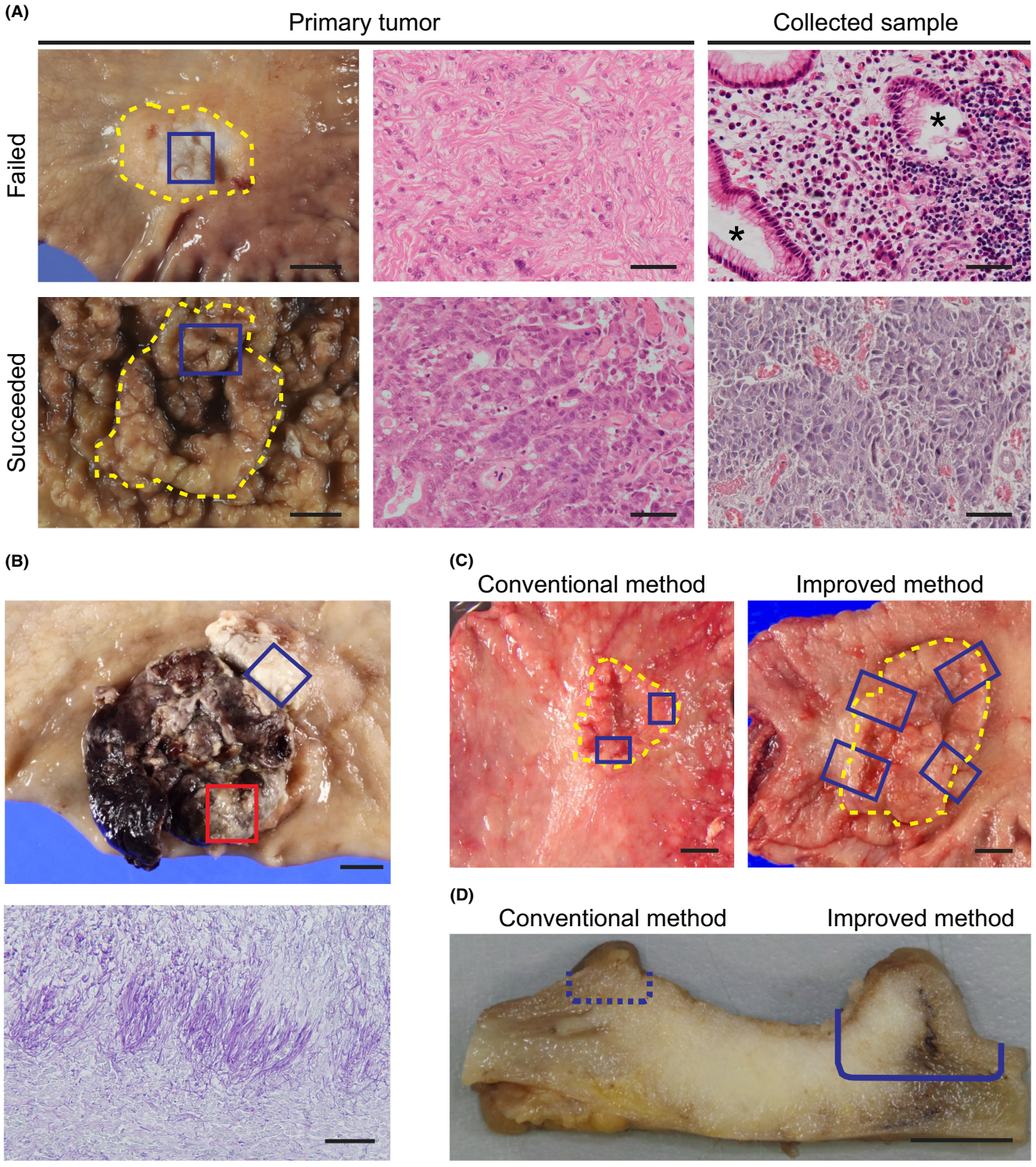

FIGURE 1 Possible reasons for unsuccessful gastric cancer stem cell (GC-SC) spheroid culture. (A) Macroscopic luminal views of the resected specimens (left) and H&E-stained sections of the primary tumors (center) and collected tissue samples (right) in a failed (top) and a succeeded (HG6T, bottom) case. Yellow dotted lines outline the tumor area. Blue boxes show the regions of sample collection. Note that a collected sample of the failed case contains non-neoplastic glandular epithelial cells (asterisks). Scale bar, 10 mm (left) and 50 μm (center and right). (B) A macroscopic view of a necrotic GC case (top) and a periodic acid–Schiff-stained section (bottom) of the collected tumor region (top, red box), showing accumulation of fungal hyphae on the surface. The blue box shows another resected region with successful spheroid culture (HG5T). Scale bar, 10 mm (top) and 50 μm (bottom). (C) Macroscopic views of representative GC cases indicating tumor regions for sample collection (blue boxes) before (conventional method, left) and after improving the method (improved method, right). Yellow dotted lines outline the tumor area. Note that wider regions across the tumor boundary were dissected for the improved method. Scale bar, 10 mm. (D) A cross-sectional view of a representative GC case indicating the depth of tumor dissection for sample collection. Cutting along a dotted line can result in missing cancer cells in the tissue sample (conventional method). The cancer tissue should be cut deeply along a solid line to obtain enough cancer stem cells (improved method). Scale bar, 5 mm.

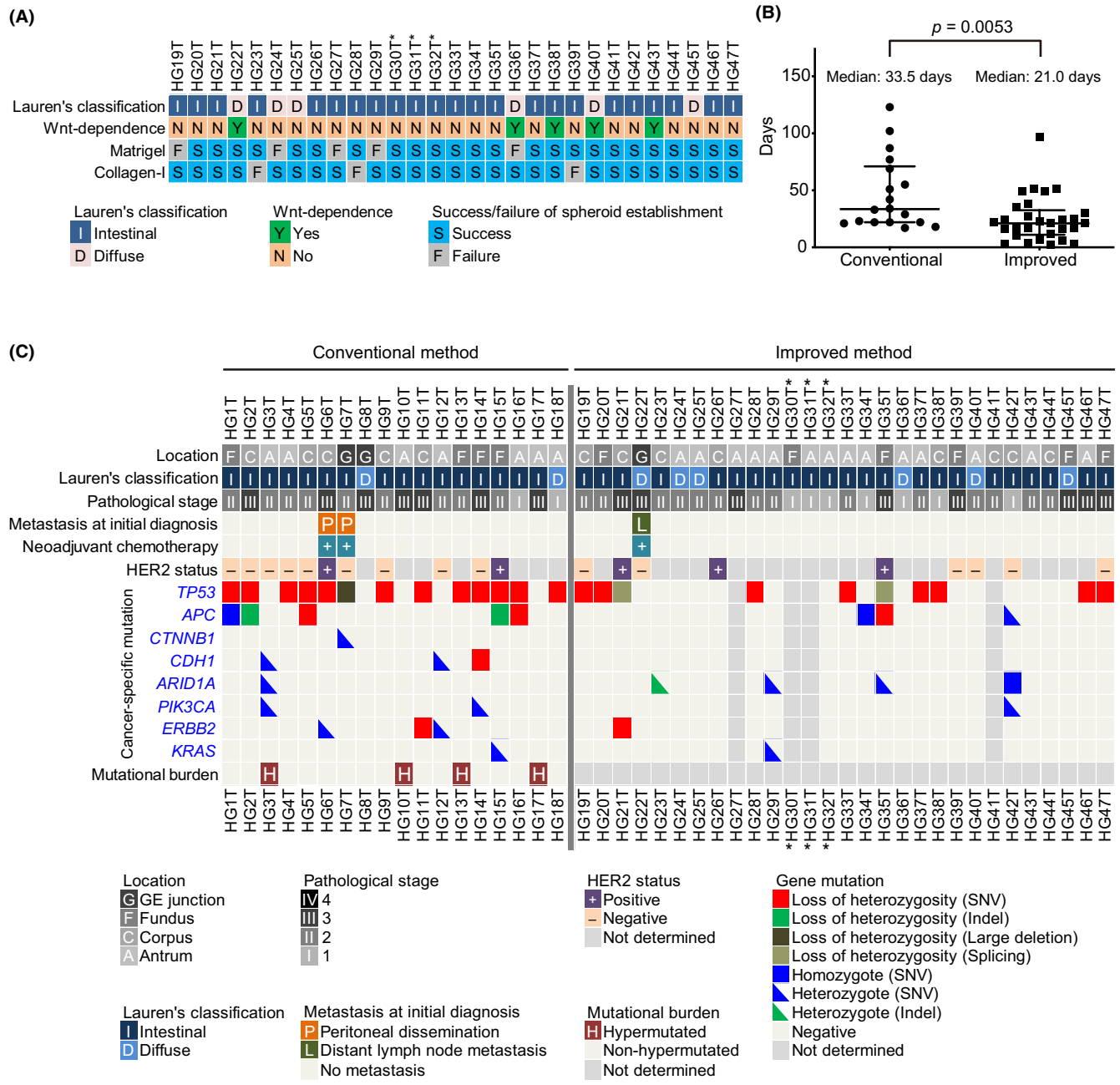

FIGURE 2 Establishment of patient-derived gastric cancer stem cell (PD–GC-SC) spheroids using an improved method. (A) Extracellular matrix (ECM) and Wnt ligand preference in primary culture. The spheroid lines were considered Wnt-dependent when they perished in the cancer medium without L-WRN CM during three serial passages. The three spheroid lines labeled with asterisks derived from a single patient. (B) Rapid establishment of GC-SC spheroids in the improved culture condition. The duration time needed for expansion of each spheroid line from the patient sample to 12 wells of a 12-well cell-culture plate is plotted with the medians and interquartile ranges. *p* value, analyzed using Mann–Whitney *U*-test. (C) Clinicopathological characteristics and mutational statuses of PD–GC-SC spheroids. Shown are pathological features of 47 lines and representative genetic alterations of 43 lines. The pathological stage was determined by examination of surgically resected specimens. The HER2 status of the primary tumor was determined by immunohistochemistry or in situ hybridization. Cancer-specific mutations were detected using a comprehensive cancer panel (HG1T–HG18T) or RNA sequencing (HG19T–HG47T). Indel, insertion/deletion variant; SNV, single nucleotide variant. The three spheroid lines labeled with asterisks derived from a single patient.

epithelial components of their primary cancer tissues (Figure S2C). Consistent with a previous study,[33] culturing a Wnt-dependent spheroid line (HG22T) in the Wnt-free cancer medium accumulated signet-ring cell-like cells that were prominent in the primary tumor (Figure S2D). To assess the tumor-initiating activity in vivo, we injected GC-SC spheroids subcutaneously into immunodeficient mice, as we reported previously.[34] Three of the five GC-SC spheroid lines formed subcutaneous tumors in nude or NSG mice, and their epithelial structures were similar to those of the primary tumors (Figure S3A,B), indicating that most of our GC-SC spheroid

lines contained abundant tumor-initiating cells. Genetic alterations of *TP53* and *APC* were detected frequently in the first patient cohort (13 and five lines, respectively, of 18), whereas they were less frequent in the second cohort (10 and three lines, respectively, of 25), suggesting that the improved culture condition helped propagate niche factor-sensitive GC-SCs that did not carry these key driver mutations (Figure 2C; Tables S4 and S5). Based on the estimated amounts of mutational burden, we identified four hypermutated GC-SC spheroid lines in the first patient cohort (22%; four of 18 lines; Figure 2C; Figure S4A), which was confirmed for lack of mismatch repair proteins by immunohistochemistry (Figure S4B,C; Table S6).

Collectively, these results demonstrated that our revised method for GC-SC spheroids was more efficient than our previous one.

3.2 | Collagen type-I stimulates the growth of some slow-growing gastric cancer stem-cell spheroids

A diffuse-type GC-SC spheroid line (HG18T) embedded in Matrigel grew very slowly in vitro compared with other lines in the first patient cohort. Diffuse-type GC cells often invade the stromal layer of gastric mucosa,[4] suggesting that these cells have a higher affinity to collagen (e.g., collagen type-I) than Matrigel extracellular scaffold rich in laminin-1.[35] Therefore, we cultured HG18T and other spheroid lines separately in Matrigel and collagen type-I. Notably, HG18T spheroids preferentially proliferated in collagen type-I, whereas HG13T and HG15T in Matrigel. Other lines, HG6T, HG14T, and HG16T, showed little differences in growth between the two matrix materials without affecting the maintenance of spheroid lines because they more than quadrupled their cell volume in 6 days in either Matrigel or collagen type-I (Figure 3A,B). Thus, we decided to try both Matrigel and collagen type-I simultaneously but separately for primary culture of PD–GC-SCs, and empirically determine the matrix best suited for each GC-SC spheroid line.

3.3 | Exogenous Wnt ligands stimulate the growth of some slow-growing gastric cancer stem-cell spheroids

Previous studies have shown that a subset of GC organoids is dependent on exogenous Wnt ligands such as Wnt and/or R-spondin for growth.[13,14] However, Wnt ligands cause predominant growth of NGE-SCs in primary culture, which necessitates another selection procedure to enrich GC-SCs.[13,14,33] To resolve this problem, we hypothesized that a low concentration of L-WRN CM that contained Wnt ligands could stimulate the growth of Wnt-responsive GC-SC spheroids without affecting NGE-SCs. Before determining such a concentration of L-WRN CM, we titrated its activity to ensure the reproducibility of culture conditions. We determined mRNA expression levels of *MKI67* (proliferation marker) and *LGR5* (stem cell marker) in normal colonic epithelial SC spheroids cultured with eL-WRN media containing serially diluted L-WRN CM according to the previous guidelines for quality control testing.[26] As a result, we found that low concentrations of L-WRN CM (1%–10%) from two different sources (in-house and commercial media) stimulated *MKI67* mRNA expression in a dose-dependent manner but failed to maintain *LGR5* mRNA levels (Figure S5). Next, we conducted serial dilutions of in-house L-WRN CM with the cancer medium in the range of 0%–20% to titrate its effects on the growth of HG13T and HG18T, which showed the lowest growth rates among our GC-SC lines that we have established so far (Figure 3B). In both spheroid lines, 5%–10% of L-WRN CM supported the proliferation of GC-SC spheroids, whereas 5% CM of NGE-SC spheroids did not (Figure 4A,B; Figure S6A–C). Interestingly, 5% L-WRN CM stimulated the expression of the stem cell marker *LGR5* in both HG13T and HG18T but not in NGE-SCs (Figure 4C). In contrast, L-WRN CM had smaller effects on the expression of the proliferation marker *MKI67* in GC-SC lines than those in NGE-SCs (Figure 4C). These results suggested that supplementation with a low concentration (e.g., at 5%) of L-WRN CM should support self-renewal of Wnt-responsive GC-SCs without allowing that of NGE-SCs.

4 | DISCUSSION

In this study, we propagated PD–GC-SCs using our spheroid culture method modified from that originally developed for PD–CRC-SCs.[21] Although non-serum culture media are commonly used for organoid culture,[36] the present method takes advantage of the serum-containing media that allow cost-efficient propagation of pure populations of normal epithelial stem cells as undifferentiated spheroids.[22,24] We previously applied this strategy to culture PD–CRC-SCs, and established more than 160 such spheroid lines at a high efficiency (up to approximately 90%).[21] Although the establishment of PD–GC-SC lines was more challenging than CRC-SC lines with the first patient cohort (25% success rate), we finally achieved a higher success rate (88%) by improving our previous culture protocol specifically for GC-SCs (Table 1).

Importantly, we experienced difficulty in localizing the GC-SCs by macroscopic observation of patient samples (Figure 1A) as well as more frequent contamination of fungi, likely *Candida* species (7%; in seven of 104 cases),[37,38] than in CRC (3%; in four of 148 cases). Therefore, we decided to sample tumor tissue pieces from a wider and deeper area, avoiding necrotic lesions as antifungal drugs appeared ineffective (Figure 1C,D).[38] We then re-evaluated culture conditions and newly employed collagen type-I matrix, which for the first time, shed light on the importance of ECM preference in the primary culture. Further studies are needed to determine the molecular features underlying the ECM preferences by GC-SC lines.

We also overcame the previously addressed limitations of GC organoid culture, including the high cost of niche factors and concomitant propagation of NGE-SCs,[18,39–41] by simply adding a low concentration of L-WRN CM, a cost-efficient source of stably active Wnt ligands (Figure S5).[26] These modifications should help propagate distinct populations of GC-SCs that exhibit different

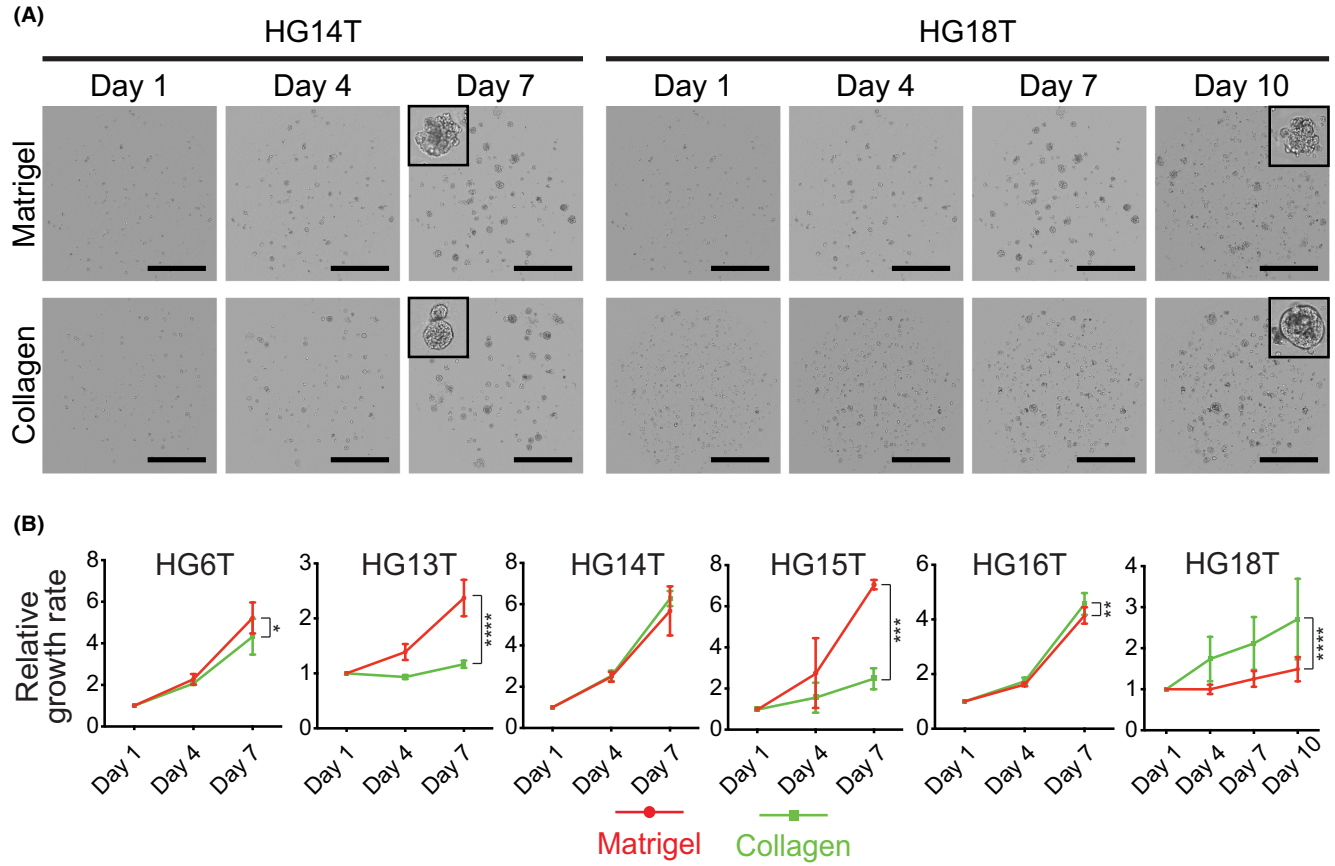

FIGURE 3 Effects of culture matrix materials on gastric cancer stem cell (GC-SC) spheroid growth. (A) Representative cell scanning images of HG14T (left) and HG18T (right) spheroids cultured in Matrigel (top) and collagen type-I (collagen, bottom). Scale bar, 1 mm. (B) Growth monitoring of spheroids with optical cell imaging. The total volumes of spheroids were estimated every 3 days during post-passage days 1 to 7 or 10. Growth rates were calibrated to the initial cell volume on day 1. Shown are the mean growth rates ± standard deviation in three independent experiments. $^{*}p < 0.05$; $^{**}p < 0.01$; $^{***}p < 0.001$; $^{****}p < 0.0001$, statistical significance of the data difference (two-way ANOVA followed by Tukey's post-test).

dependencies on the niche factors without the need for negative selection to eliminate NGE-SCs.

In conclusion, we developed a simple and efficient method to propagate PD–GC-SC spheroids by improving our conventional sample collection protocol and culture conditions. Recent studies have shown that the drug sensitivity test on PD-CRC organoids can predict patient outcomes with 100% sensitivity,[42,43] even if some intra-tumor heterogeneity is lost in the spheroid/organoid line.[44] Our PD–GC-SC spheroids can be utilized to investigate new molecular targeted therapies and their companion diagnostics for patient selection,[45,46] as we recently identified a subset of PD–CRC-SC spheroid lines that responded to fibroblast growth factor receptor inhibitors.[47,48] Additionally, the genomic and expression profiles of GC-SC spheroids will help determine novel molecular subtypes and diagnostic gene signatures. Thus, our improved method may open a new horizon for personalized GC diagnosis and treatment.

AUTHOR CONTRIBUTIONS

Conception and design, T. Morimoto (TMo), MMT, and H. Miyoshi (HMi); Development of methodology, TMo, YT, T. Miura (TMi), and HMi; Investigation, TMo, T. Yamamoto, FK, HA, H. Maekawa (HMa), T. Yamaura, and HMi; Analysis and interpretation of data, TMo, YT, TMi, and HMi; Administrative and material support, HMa, KK, YS, YY, HT, and KO; Manuscript writing, TMo, MMT, and HMi.

ACKNOWLEDGMENTS

The authors thank members of the Department of Surgery at KUHP and Medical Research Institute Kitano Hospital for help collecting surgical specimens; Hiromi Kikuchi for technical assistance; and the Medical Research Support Center, Graduate School of Medicine, Kyoto University for the use of the facility. We also thank Dr. Thaddeus S. Stappenbeck for providing L-WRN cells. We are grateful to Dr. Masanobu Oshima for comments on the manuscript.

FUNDING INFORMATION

This work was supported by Grants-in-Aid for Scientific Research (JP18H02639 and JP22K07187 to H.Miyoshi and JP21K06948 to FK) from the Japan Society for the Promotion of Science; research funds from Kyo Diagnostics K.K. and SCREEN Holdings Co., Ltd. (to H.Miyoshi and KO); the Program for Creating Start-ups from Advanced Research and Technology (ST261001TT) from the Japan

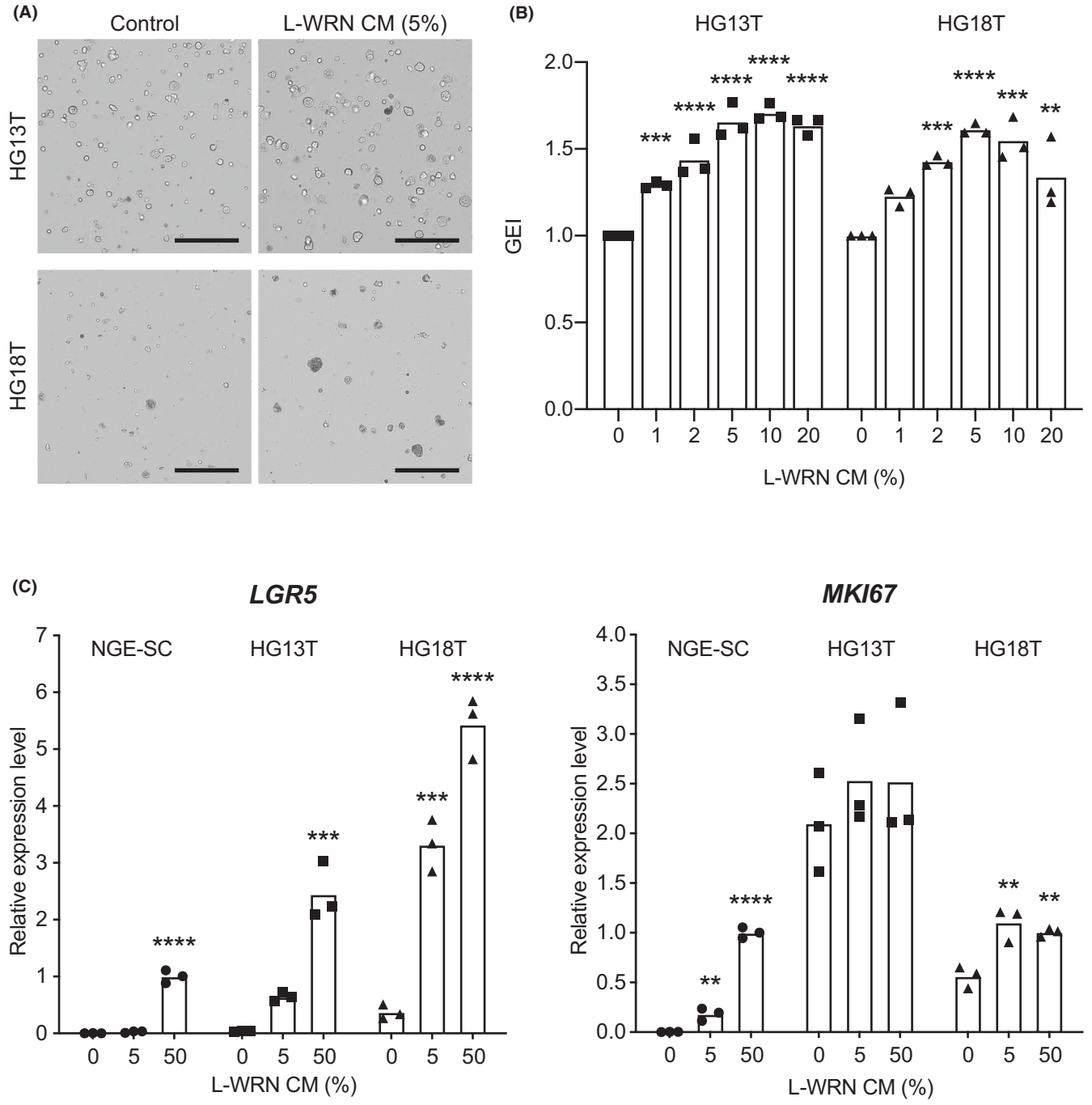

FIGURE 4 Effects of L-WRN conditioned medium (CM) on gastric cancer stem cell (GC-SC) spheroid growth. (A) Representative cell scanning images of HG13T (top) and HG18T (bottom) spheroids cultured with (right) and without (control, left) 5% L-WRN CM for 6 days. Scale bar, 1 mm. (B) Growth monitoring of HG13T (left) and HG18T (right) spheroids with optical cell imaging. The GEI were calculated based on the growth rate of untreated spheroids (0%). The GEI in three independent experiments are plotted with the means. (C) Expression levels of *LGR5* (left) and *MKI67* (right) mRNAs determined by quantitative RT-PCR analysis. Normal gastric epithelial stem cell (NGE-SC) and GC-SC (HG13T and HG18T) spheroids were cultured in the cancer media containing 0%, 5%, or 50% L-WRN CM for 3 days. Relative expression levels in three independent experiments are plotted with the means. $^{**}p<0.01$; $^{***}p<0.001$; $^{****}p<0.0001$, statistical significance of the data difference between untreated (0%) and treated groups (one-way ANOVA followed by Tukey's post-test).

Science and Technology Agency (to MMT); the Practical Research for Innovative Cancer Control (ck0106195h) from the Japan Agency for Medical Research and Development (to MMT); the Kyoto University Venture Incubation from the Kyoto University Office of Society-Academia Collaboration for Innovation (to MMT); and the Dynamic Project for Colon Cancer Personalized Therapy from the Institute for Advancement of Clinical and Translational Science, KUHP (to MMT).

CONFLICT OF INTEREST STATEMENT

H. Miyoshi and KO received research funds from Kyo Diagnostics K.K. and SCREEN Holdings. MMT owns stock in Kyo Diagnostics K.K. YT and H.Maekawa belong to the Department of Personalized Cancer Medicine at the Graduate School of Medicine, Kyoto University, which is supported by Kyo Diagnostics K. K., AFI, and SCREEN Holdings. T.Miura is an employee of SCREEN Holdings. The other authors have no conflicts of interest to declare.

ETHICS STATEMENTS

Approval of the research protocol by an Institutional Reviewer Board: The study protocol was approved by Kyoto University Graduate School and Faculty of Medicine, Ethics Committee (No. R0915 and R0857) as well as that of Medical Research Institute Kitano Hospital (extension of the Kyoto University study as a collaboration).

Informed Consent: Written informed consent was obtained from all patients.

Registry and the Registration No. of the study/trial: N/A.

Animal Studies: All animal experiments were conducted according to the protocol approved by the Institutional Animal Care and Use Committee of Kyoto University Graduate School of Medicine (Nos 14546, 15091, 16047, 16654, 17086, 18080, and 19601).

ORCID

Tomonori Morimoto https://orcid.org/0000-0003-0535-0889
Yukitoshi Takemura https://orcid.org/0000-0003-3066-6658
Takemitsu Miura https://orcid.org/0000-0003-4565-529X
Takehito Yamamoto https://orcid.org/0000-0002-2236-7124
Fumihiko Kakizaki https://orcid.org/0000-0003-2017-6700
Hideo An https://orcid.org/0009-0004-4762-7617
Hisatsugu Maekawa https://orcid.org/0000-0002-0200-414X
Tadayoshi Yamaura https://orcid.org/0000-0003-0019-1313
Kenji Kawada https://orcid.org/0000-0003-4336-6937
Yoshiharu Sakai https://orcid.org/0000-0001-9864-4186
Hiroaki Terajima https://orcid.org/0000-0001-7938-6345
Kazutaka Obama https://orcid.org/0000-0003-2924-6701
Makoto Mark Taketo https://orcid.org/0000-0002-9032-4505
Hiroyuki Miyoshi https://orcid.org/0000-0001-7400-0714

REFERENCES

1. Sung H, Ferlay J, Siegel RL, et al. Global Cancer Statistics 2020: GLOBOCAN estimates of incidence and mortality worldwide for 36 cancers in 185 countries. *CA Cancer J Clin*. 2021;71:209-249.
2. Joshi SS, Badgwell BD. Current treatment and recent progress in gastric cancer. *CA Cancer J Clin*. 2021;71:264-279.
3. Lauren P. The two histological main types of gastric carcinoma: Diffuse and so-called intestinal-type carcinoma. An attempt at a histo-clinical classification. *Acta Pathol Microbiol Scand*. 1965;64:31-49.
4. Lokuhetty D, White AV, Watanabe R, Cree AI. *Digestive system tumours: WHO classification of tumours*. 5th ed. IARC; 2019.
5. Cancer Genome Atlas Research Network. Comprehensive molecular characterization of gastric adenocarcinoma. *Nature*. 2014;513:202-209.
6. Cristescu R, Lee J, Nebozhyn M, et al. Molecular analysis of gastric cancer identifies subtypes associated with distinct clinical outcomes. *Nat Med*. 2015;21:449-456.
7. Bang YJ, Van Cutsem E, Feyereislova A, et al. Trastuzumab in combination with chemotherapy versus chemotherapy alone for treatment of HER2-positive advanced gastric or gastro-oesophageal junction cancer (ToGA): a phase 3, open-label, randomised controlled trial. *Lancet*. 2010;376:687-697.
8. Roviello G, Corona SP, D'Angelo A, Rosellini P, Nobili S, Mini E. Immune checkpoint inhibitors in pre-treated gastric cancer patients: results from a literature-based meta-analysis. *Int J Mol Sci*. 2020;21:448.
9. Pietrantonio F, Randon G, Di Bartolomeo M, et al. Predictive role of microsatellite instability for PD-1 blockade in patients with advanced gastric cancer: a meta-analysis of randomized clinical trials. *ESMO Open*. 2021;6:100036.
10. Fujii M, Matano M, Nanki K, Sato T. Efficient genetic engineering of human intestinal organoids using electroporation. *Nat Protoc*. 2015;10:1474-1485.
11. Seino T, Kawasaki S, Shimokawa M, et al. Human pancreatic tumor organoids reveal loss of stem cell niche factor dependence during disease progression. *Cell Stem Cell*. 2018;22:454-467.e456.
12. Sato T, Stange DE, Ferrante M, et al. Long-term expansion of epithelial organoids from human colon, adenoma, adenocarcinoma, and Barrett's epithelium. *Gastroenterology*. 2011;141:1762-1772.
13. Nanki K, Toshimitsu K, Takano A, et al. Divergent routes toward Wnt and R-spondin niche independency during human gastric carcinogenesis. *Cell*. 2018;174:856-869.e817.
14. Yan HHN, Siu HC, Law S, et al. A comprehensive human gastric cancer organoid biobank captures tumor subtype heterogeneity and enables therapeutic screening. *Cell Stem Cell*. 2018;23:882-897.e811.
15. Gao M, Lin M, Rao M, et al. Development of patient-derived gastric cancer organoids from endoscopic biopsies and surgical tissues. *Ann Surg Oncol*. 2018;25:2767-2775.
16. Seidlitz T, Merker SR, Rothe A, et al. Human gastric cancer modelling using organoids. *Gut*. 2019;68:207-217.
17. Steele NG, Chakrabarti J, Wang J, et al. An organoid-based preclinical model of human gastric cancer. *Cell Mol Gastroenterol Hepatol*. 2019;7:161-184.
18. Wuputra K, Ku CC, Kato K, Wu DC, Saito S, Yokoyama KK. Translational models of 3-D organoids and cancer stem cells in gastric cancer research. *Stem Cell Res Ther*. 2021;12:492.
19. Li G, Ma S, Wu Q, et al. Establishment of gastric signet ring cell carcinoma organoid for the therapeutic drug testing. *Cell Death Discov*. 2022;8:6.
20. Song H, Park JY, Kim JH, et al. Establishment of patient-derived gastric cancer organoid model from tissue obtained by endoscopic biopsies. *J Korean Med Sci*. 2022;37:e220.
21. Miyoshi H, Maekawa H, Kakizaki F, et al. An improved method for culturing patient-derived colorectal cancer spheroids. *Oncotarget*. 2018;9:21950-21964.
22. Miyoshi H, Stappenbeck TS. In vitro expansion and genetic modification of gastrointestinal stem cells in spheroid culture. *Nat Protoc*. 2013;8:2471-2482.
23. VanDussen KL, Marinshaw JM, Shaikh N, et al. Development of an enhanced human gastrointestinal epithelial culture system to facilitate patient-based assays. *Gut*. 2015;64:911-920.
24. Wilson SS, Mayo M, Melim T, et al. Optimized culture conditions for improved growth and functional differentiation of mouse and human colon organoids. *Front Immunol*. 2020;11:547102.
25. Stelzner M, Helmrath M, Dunn JC, et al. A nomenclature for intestinal in vitro cultures. *Am J Physiol Gastrointest Liver Physiol*. 2012;302:G1359-G1363.
26. VanDussen KL, Sonnek NM, Stappenbeck TS. L-WRN conditioned medium for gastrointestinal epithelial stem cell culture shows

replicable batch-to-batch activity levels across multiple research teams. *Stem Cell Res*. 2019;37:101430.
27. Yamaura T, Miyoshi H, Maekawa H, et al. Accurate diagnosis of mismatch repair deficiency in colorectal cancer using high-quality DNA samples from cultured stem cells. *Oncotarget*. 2018;9:37534-37548.
28. Reiter JG, Baretti M, Gerold JM, et al. An analysis of genetic heterogeneity in untreated cancers. *Nat Rev Cancer*. 2019;19:639-650.
29. Danecek P, Auton A, Abecasis G, et al. The variant call format and VCFtools. *Bioinformatics*. 2011;27:2156-2158.
30. Wang K, Li M, Hakonarson H. ANNOVAR: functional annotation of genetic variants from high-throughput sequencing data. *Nucleic Acids Res*. 2010;38:e164.
31. Narahara M, Higasa K, Nakamura S, et al. Large-scale East-Asian eQTL mapping reveals novel candidate genes for LD mapping and the genomic landscape of transcriptional effects of sequence variants. *PLoS ONE*. 2014;9:e100924.
32. Higasa K, Miyake N, Yoshimura J, et al. Human genetic variation database, a reference database of genetic variations in the Japanese population. *J Hum Genet*. 2016;61:547-553.
33. Togasaki K, Sugimoto S, Ohta Y, et al. Wnt signaling shapes the histologic variation in diffuse gastric cancer. *Gastroenterology*. 2021;160:823-830.
34. Maekawa H, Miyoshi H, Yamaura T, et al. A chemosensitivity study of colorectal cancer using xenografts of patient-derived tumor-initiating cells. *Mol Cancer Ther*. 2018;17:2187-2196.
35. Moreira AM, Pereira J, Melo S, et al. The extracellular matrix: an accomplice in gastric cancer development and progression. *Cell*. 2020;9:394.
36. Drost J, Clevers H. Organoids in cancer research. *Nat Rev Cancer*. 2018;18:407-418.
37. Eras P, Goldstein MJ, Sherlock P. Candida infection of the gastrointestinal tract. *Medicine (Baltimore)*. 1972;51:367-379.
38. Katzenstein AL, Maksem J. Candidal infection of gastric ulcers. Histology, incidence, and clinical significance. *Am J Clin Pathol*. 1979;71:137-141.
39. Dedhia PH, Bertaux-Skeirik N, Zavros Y, Spence JR. Organoid models of human gastrointestinal development and disease. *Gastroenterology*. 2016;150:1098-1112.
40. Seidlitz T, Stange DE. Gastrointestinal cancer organoids-applications in basic and translational cancer research. *Exp Mol Med*. 2021;53:1459-1470.
41. Pang MJ, Burclaff JR, Jin R, et al. Gastric organoids: progress and remaining challenges. *Cell Mol Gastroenterol Hepatol*. 2022;13:19-33.
42. Vlachogiannis G, Hedayat S, Vatsiou A, et al. Patient-derived organoids model treatment response of metastatic gastrointestinal cancers. *Science*. 2018;359:920-926.
43. Ooft SN, Weeber F, Dijkstra KK, et al. Patient-derived organoids can predict response to chemotherapy in metastatic colorectal cancer patients. *Sci Transl Med*. 2019;11:eaay2574.
44. Roerink SF, Sasaki N, Lee-Six H, et al. Intra-tumour diversification in colorectal cancer at the single-cell level. *Nature*. 2018;556:457-462.
45. Choi S, Park S, Kim H, Kang SY, Ahn S, Kim KM. Gastric cancer: mechanisms, biomarkers, and therapeutic approaches. *Biomedicine*. 2022;10:543.
46. Li T, He Y, Zhong Q, Yu J, Chen X. Advances in treatment models of advanced gastric cancer. *Technol Cancer Res Treat*. 2022;21:153303382210903.
47. Yamamoto T, Miyoshi H, Kakizaki F, et al. Chemosensitivity of patient-derived cancer stem cells identifies colorectal cancer patients with potential benefit from FGFR inhibitor therapy. *Cancers (Basel)*. 2020;12:2010.
48. Kitano S, Yamamoto T, Taketo MM. Novel parameter for cancer chemosensitivity to fibroblast growth factor receptor inhibitors. *Cancer Sci*. 2022;113:4005-4010.

SUPPORTING INFORMATION

Additional supporting information can be found online in the Supporting Information section at the end of this article.

How to cite this article: Morimoto T, Takemura Y, Miura T, et al. Novel and efficient method for culturing patient-derived gastric cancer stem cells. *Cancer Sci*. 2023;00:1-11. doi:10.1111/cas.15840

Supplementary Materials and Methods

Morphological observation of spheroids

Phase-contrast images of spheroids were captured using an Olympus IX70 microscope equipped with an Olympus DP70 digital camera (Olympus, Tokyo, Japan).

Preparation of DNA and histology specimens of spheroids

Spheroids in Matrigel were suspended in Cell Recovery Solution (Corning), and they were incubated at 4°C for 30–60 min. Spheroids in collagen type-I were suspended in collagenase solution, and they were incubated at 37°C for 30 min. Next, the spheroids were centrifuged at 200 × *g* for 5 min and washed with PBS. Genomic DNA was purified using a DNeasy Blood & Tissue Kit (Qiagen, Venlo, the Netherlands). For histological analyses, spheroids were embedded in iPGell (Genostaff, Tokyo, Japan) and fixed with 4% paraformaldehyde in PBS at 4°C for 3 days.

Patient-derived spheroid xenograft (PDSX)

Four- to six-week-old female nude and NSG mice were purchased from The Jackson Laboratory Japan (Yokohama, Japan). The spheroid suspension was subcutaneously injected into mice as

described previously.[34]

Histopathological classification of gastric cancer

Formalin-fixed, paraffin-embedded specimens were sectioned into 4-μm thick sections, and they were stained with H&E. Histological images were captured using a Leica DM2000 microscope (Leica, Wetzlar, Germany) equipped with an Olympus DP73 digital camera (Olympus), and histological grades of primary tumors and spheroids were determined according to the 5th edition of WHO guidelines.[4]

Immunohistochemistry

Primary antibodies against MLH-1 (M1, Ventana, Oro Valley, AZ, USA), PMS2 (EPR 3947, Ventana), MSH2 (G219-1129, Ventana), MSH6 (EPR3945, Abcam, Cambridge, UK), Ki67 (SP6, ThermoFisher, Waltham, MA, USA), CDX2 (SM392-5M, BioiGenex, Fremont, CA, USA), and MUC2 (CCP58, Agilent, Santa Clara, CA, USA) were purchased from commercial sources. Deparaffinized sections were incubated in Trilogy solution (Sigma-Aldrich) at 95°C for 60 min for unmasking target antigens, and they were further incubated in 0.3% H_2O_2 in methanol to inactivate endogenous peroxidases at room temperature for 15 min. Primary antibodies diluted in the blocking buffer [5% goat serum (Vector Laboratories, Burlingame, CA, USA) and 3%

bovine serum albumin (Sigma-Aldrich) in PBS] were applied on the sections. Specific signals were visualized using OptiView DAB IHC Detection Kit (Ventana) or the VECTASTAIN Elite ABC Kit (Vector Laboratories).

Quantitative RT-PCR (qRT-PCR)

First strand cDNA was synthesized using ReverTra Ace kit (TOYOBO, Osaka, Japan), and qPCR was performed using SYBR qPCR Mix (TOYOBO) on an StepOnePlus thermal cycler (ThermoFisher). Expression levels were normalized relative to those of *ACTB*. Sequences of primer pairs were as follows: *MKI67*, TCCTTTGGTGGGCACCTAAGACCTG and TGATGGTTGAGGTCGTTCCTTGATG; *LGR5*, CCTTCATAAGAAAGATGCTGGAA and GTTTAATGGGGGAAATGTACAGA; *ACTB*, GGGGTGTTGAAGGTCTCAAA and GGCATCCTCACCCTGAAGTA.

Supplementary figure 1: A schematic workflow for monitoring cell growth using optical cell imaging.

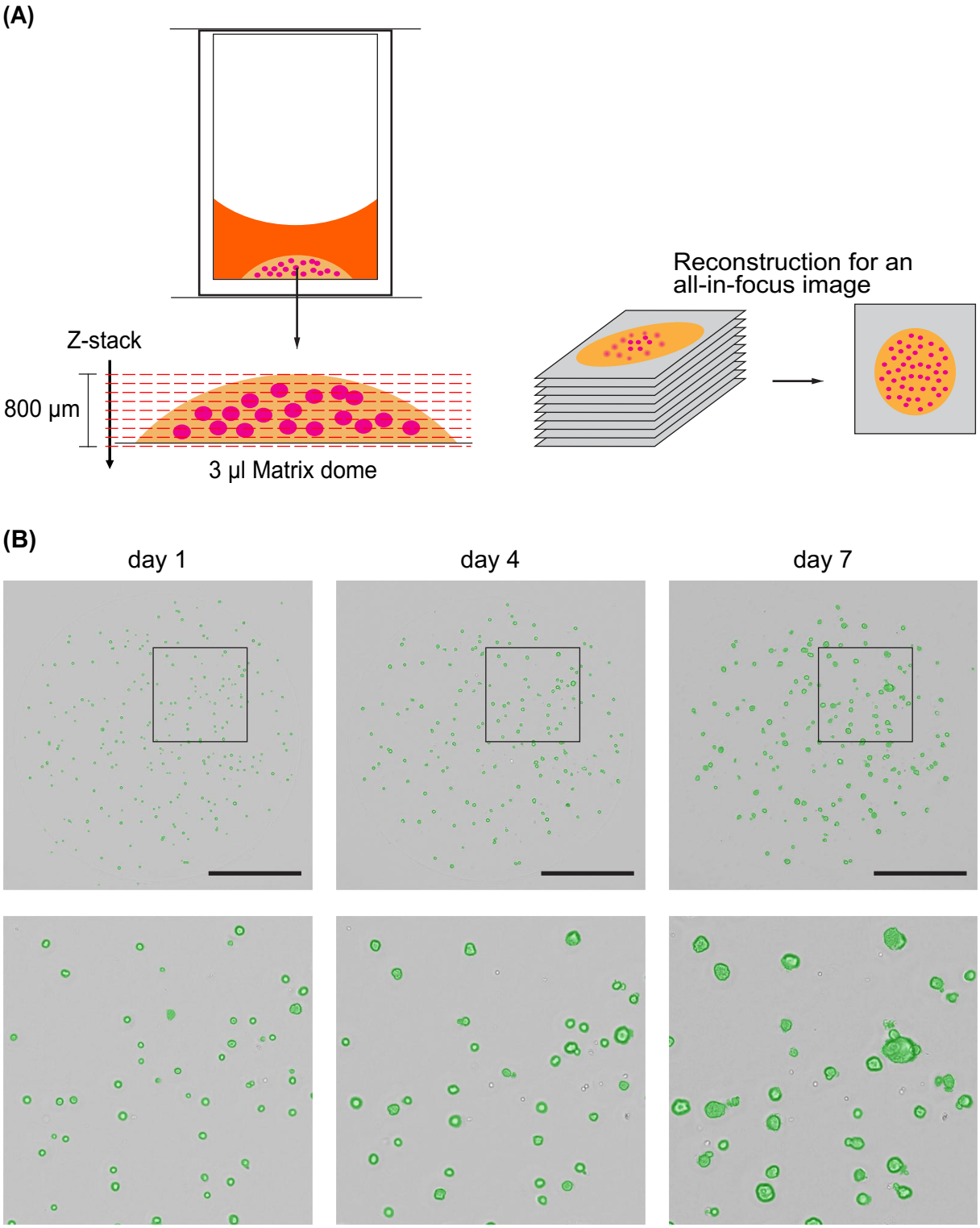

(**A**) Outline of the cell scanning procedures. Nine Z-stack images were acquired for each matrix dome (3 μL), and they were reconstructed to generate an all-in-focus image. (**B**) Time course of the spheroid growth. Shown are the reconstituted images of HG16T spheroids (top) and their higher magnification (bottom) at 1, 4, and 7 days after passage. Object areas recognized as spheroids are shown in green. Scale bar, 1 mm.

Supplementary figure 2: Histopathological characterization of patient-derived gastric cancer stem cell (PD–GC-SC) spheroids.

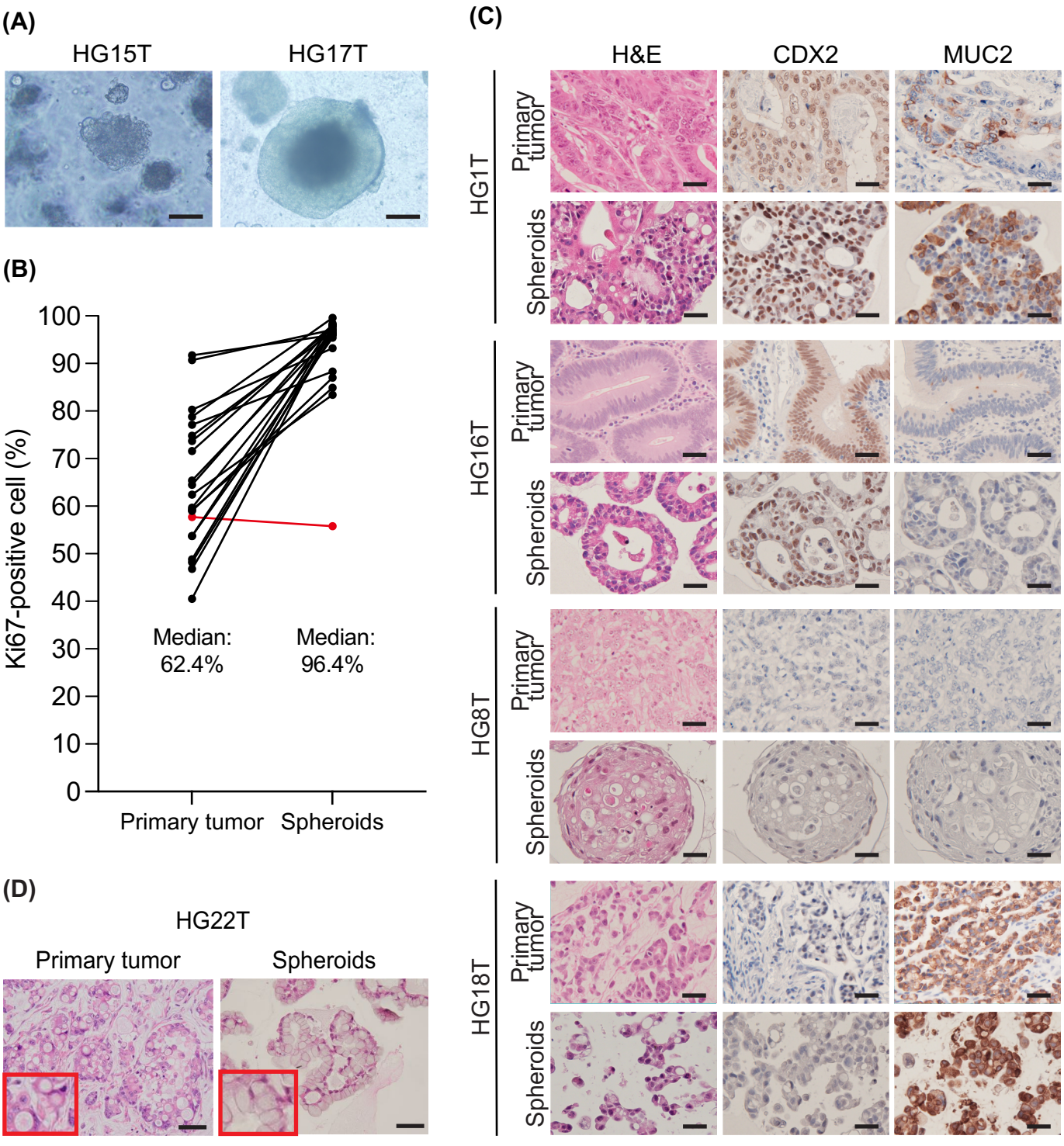

(**A**) Representative phase-contrast micrographs of GC-SC spheroids. Scale bar, 200 μm. (**B**) The fraction of proliferating cells monitored by immunohistochemistry for Ki67. The average percentages of Ki67-positiive cells in three microscopic fields are shown as raw data points with lines connecting the pairs of the primary tumors and spheroids from the same GC patients (n = 21). Note that proliferating cells were enriched in spheroids more than in primary tumors in all cases except for one diffuse-type tumor (HG8T, red). $P < 0.0001$, statistical significance of the data difference (Wilcoxon test). (**C**) Pairs of the primary tumor (top) and spheroid specimens (bottom) from the same GC patients analyzed by H&E staining (left), and by immunohistochemistry for CDX2 (center) and MUC2 (right). HG1T, tubular adenocarcinoma containing CDX2-positive moderately differentiated tumor cells forming the tubular structure. HG16T, tubular adenocarcinoma containing CDX2-positive well-differentiated tumor cells forming the tubular structure. MUC2-positive cells were heterogeneously distributed in HG1T but rarely observed in HG16T. HG8T, poorly cohesive carcinoma containing CDX2-negative/MUC2-negative poorly differentiated tumor cells. HG18T, mucinous adenocarcinoma containing CDX2-low/MUC2-positive poorly differentiated tumor cells. Scale bar, 50 μm. (**D**) A pair of H&E-stained specimens of the primary tumor (left) and spheroids (right) from the same GC patient (HG22T, poorly cohesive carcinoma with signet-ring cells). Spheroids were cultured in the cancer medium without L-WRN conditioned medium for three days. Insets indicate cells with large vacuoles and compressed nuclei. Scale bar, 50 μm.

Supplementary figure 3: Characterization of tumor-initiating gastric cancer (GC) cells in patient-derived spheroid xenograft (PDSX) tumors.

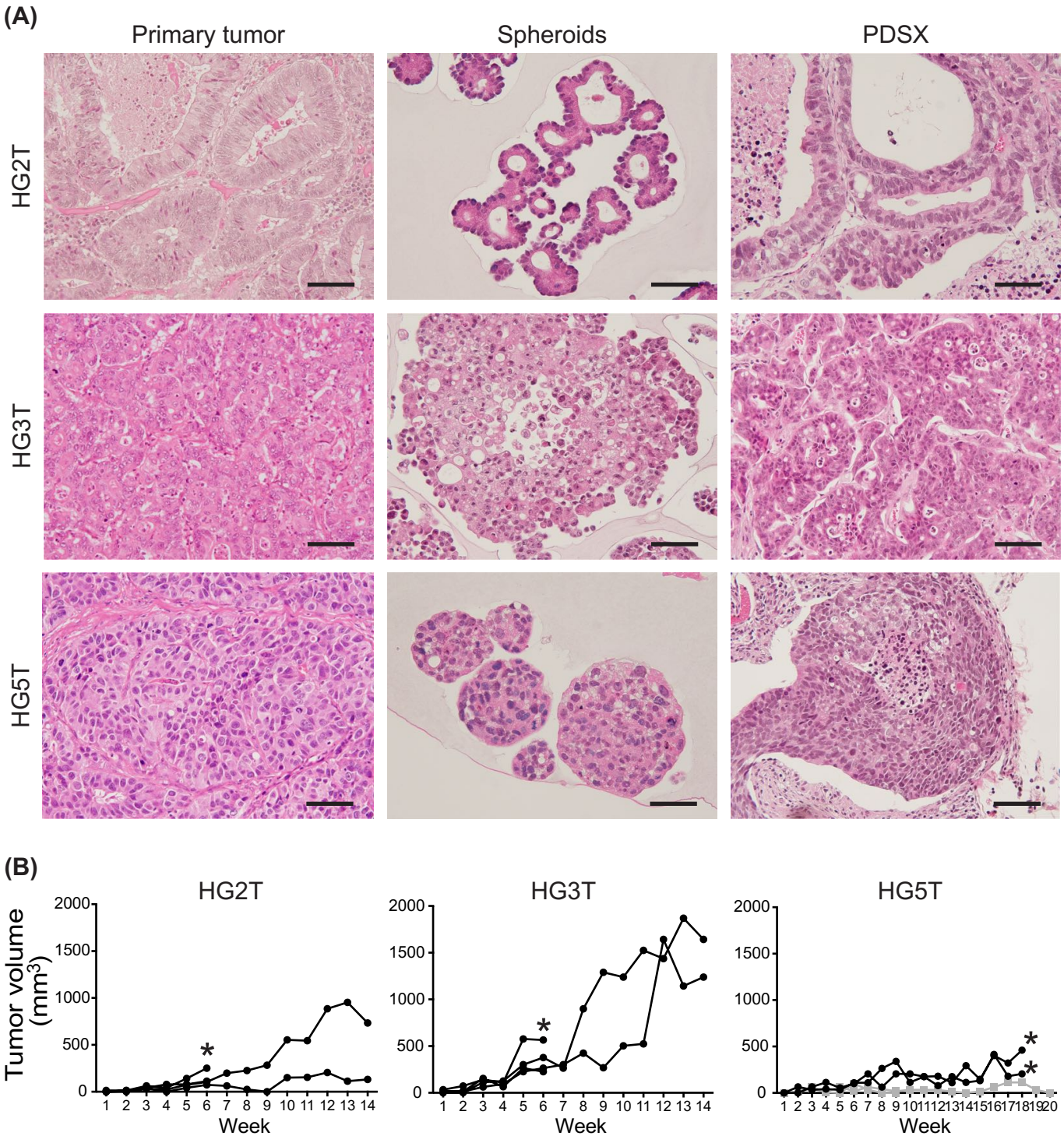

(**A**) Pairs of the primary tumor (left), spheroids (center), and PDSX specimens (right) from the same patients analyzed by H&E staining. HG2T, tubular adenocarcinoma containing well-differentiated tumor cells forming the tubular structure. HG3T, tubular adenocarcinoma containing moderately differentiated cells forming the tubular structure. HG5T, tubular adenocarcinoma containing poorly differentiated cells forming the solid structure. Scale bar, 50 μm. (**B**) Growth curves of PDSX tumors derived from GC spheroids, HG2T (n = 3), HG3T (n = 3), and HG5T (n = 4). Mice were sacrificed when they became moribund (asterisks). The tumor regressed in two PDSX mice for HG5T (gray lines).

Supplementary figure 4: Detection of mismatch repair deficiency in gastric stem cell (GC-SC) spheroids.

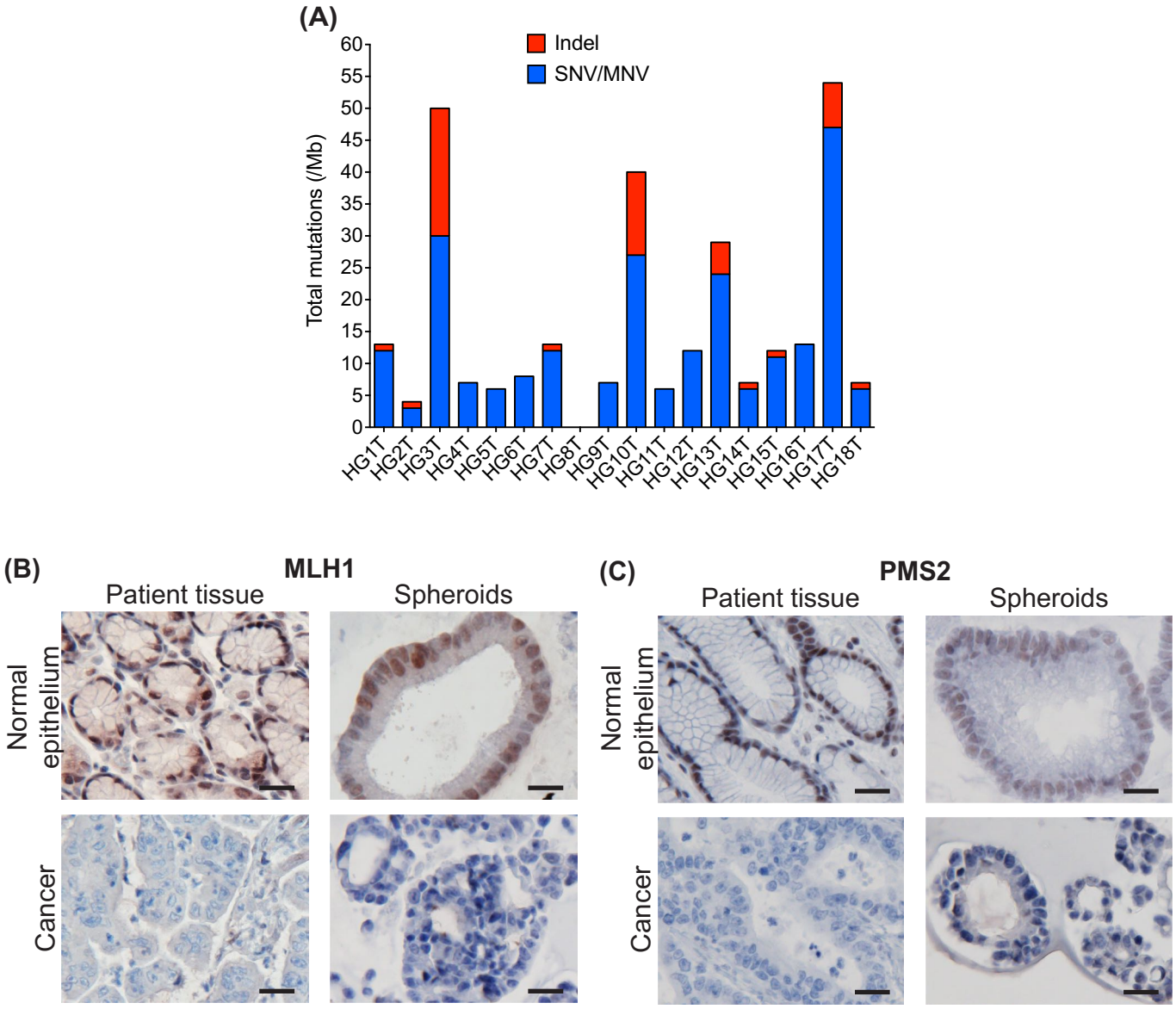

(**A**) Mutational burden estimated by exonic sequencing of 409 cancer-related genes spanning 1.29 Mb. Indel, insertion/deletion variant. SNV/MNV, single nucleotide variant/multi-nucleotide variant. (**B, C**) Immunohistochemistry for mismatch repair proteins, MLH1 (B) and PMS2 (C). Shown are paired specimens of the patient tissue (left) and spheroids (right) of the normal gastric epithelium (top) and GC (bottom) derived from the same patient (HG10T). Scale bar, 25 μm.

Supplementary figure 5: Dose-dependent effects of L-WRN conditioned media (CM) on gene expression in normal colonic epithelial stem cell (NCE-SC) spheroids.

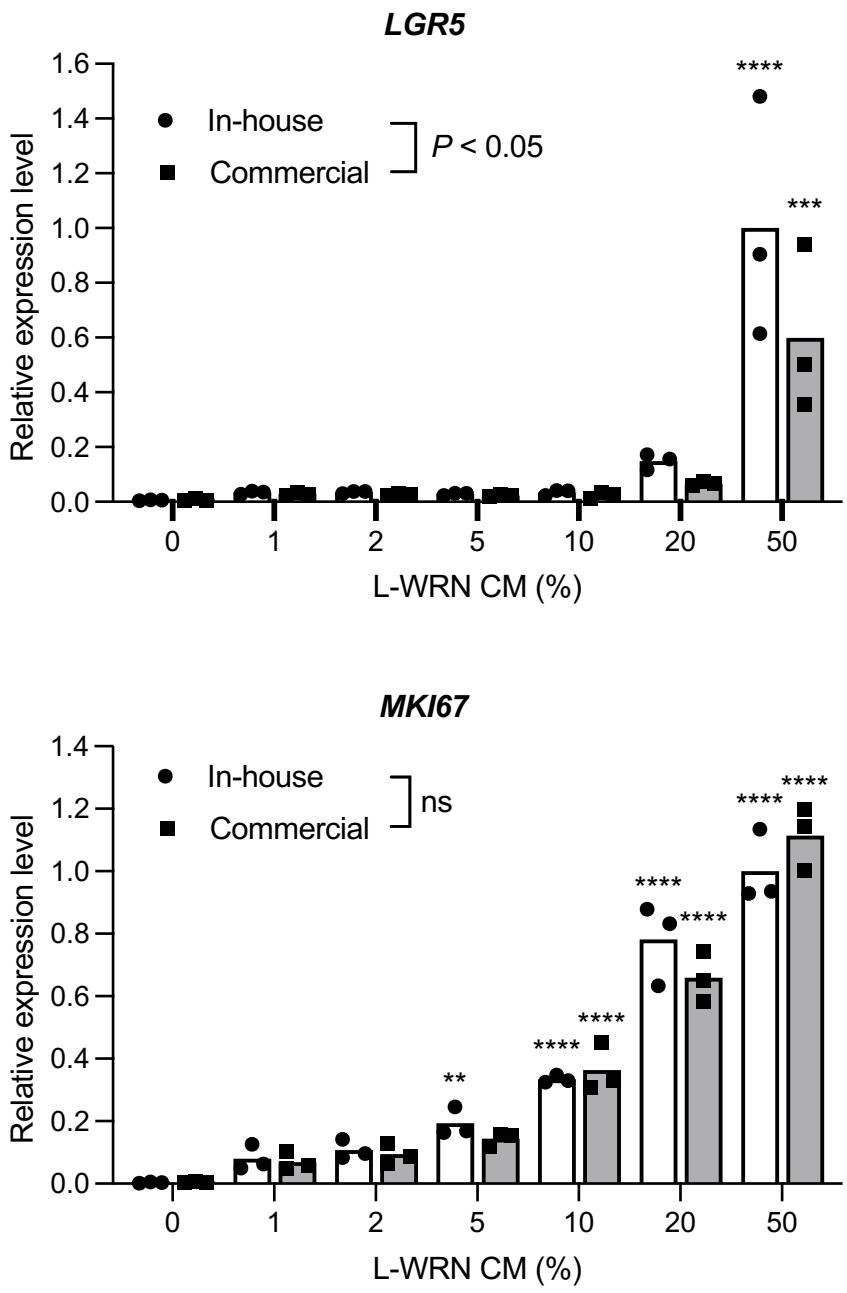

NCE-SC spheroids were cultured for 3 days in the eL-WRN media containing indicated percentages of L-WRN CM from two different sources (in-house and commercial). Plots with the means of relative expression levels of LGR5 (top) and MKI67 (bottom) were determined by qRT-PCR analysis. ***P* < 0.01; ****P* < 0.001; *****P* < 0.0001, statistical significance of the data difference between untreated (0%) and treated groups in three independent experiments (two-way ANOVA followed by Šidák's post-test).

Supplementary figure 6: Effects of L-WRN conditioned medium (CM) concentrations on the growth of normal gastric epithelial stem cells (NGE-SCs).

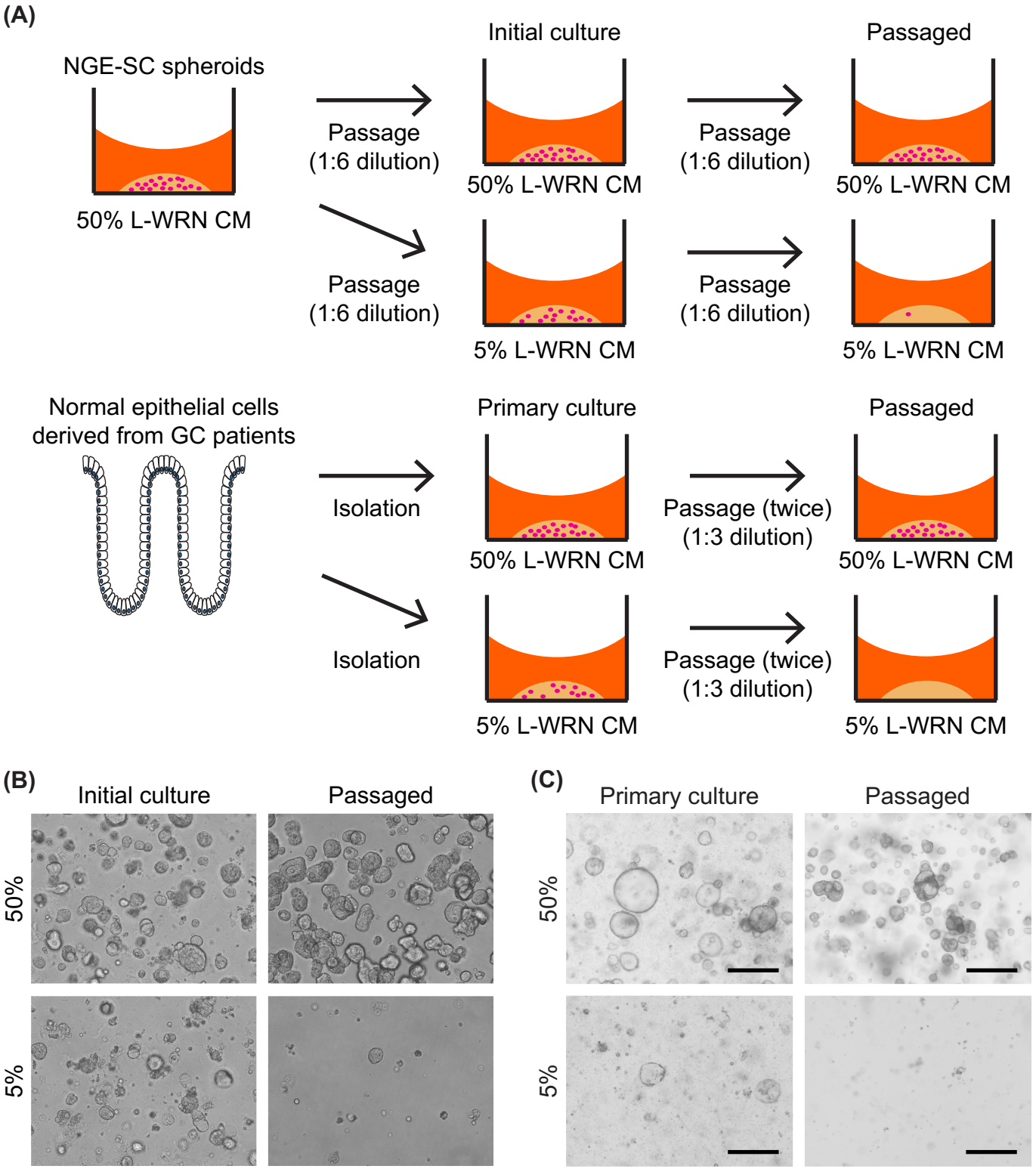

(**A**) Schematic of the experimental procedure. (**B**) NGE-SC spheroids were cultured in the cancer medium containing 50% (top) or 5% (bottom) L-WRN CM for 3 days (left; Initial culture), passaged at a split ratio of 1:6, and cultured for another 3 days (right; Passaged). Scale bar, 200 μm. (**C**) Normal gastric epithelial cells isolated from patient samples were cultured in the cancer medium containing 50% (top) or 5% (bottom) L-WRN CM for 6 days (left; Primary culture). Then spheroids were cultured for another 12 days with two serial passages at a split ratio of 1:3 (right; Passaged). Scale bar, 200 μm.

Supplementary table 1: Composition of media.

Reagent	Final conc.	Source
Washing medium		
DMEM/F12 with HEPES and L-glutamine		Nacalai Tesque
Penicillin-streptomycin solution (100 x)	1 x	Nacalai Tesque
Calf serum	10%	Sigma-Aldrich
Collagenase solution		
Washing medium		
Collagenase type I	0.2%	Thermo Fisher
Gentamicin	50 µg/ml	Thermo Fisher
Cancer medium		
Advanced DMEM/F-12		Thermo Fisher
Penicillin-streptomycin solution (100 x)	1 x	Nacalai Tesque
L-Glutamine	2 mM	Nacalai Tesque
Y27632	10 µM	R&D systems
SB431542	1 µM	R&D systems
Plasmocin	5 µg/ml	Invivogen
Fetal bovine serum	5%	Thermo Fisher
Epidermal growth factor (EGF)	50 ng/ml	Peprotech
Fibroblast growth factor 2 (FGF2)	100 ng/ml	Peprotech
5'-(*N*-Ethyl-carboxamido)-adenosine (NECA)	1 µM	Sigma-Aldrich
B27 supplement (50 x)	1 x	Thermo Fisher
L-WRN conditioned medium[a]	5%	In-house[b]
[a]L-WRN conditioned medium was added after the protocol revision.		
[b]Also available from Sigma-Aldrich (SCM105)		
eL-WRN medium		
Advanced DMEM/F-12		Thermo Fisher
Penicillin-streptomycin solution (100 x)	1 x	Nacalai Tesque
L-Glutamine	2 mM	Nacalai Tesque
L-WRN conditioned medium	50%	In-house[b]
Y27632	10 µM	R&D systems
SB431542	1 µM	R&D systems
Plasmocin	5 µg/ml	Invivogen
Fetal bovine serum	20%	Thermo Fisher
Epidermal growth factor (EGF)	50 ng/ml	Peprotech

Supplementary table 2: Success rates for spheroid establishment according to the clinicopathological characteristics of patients in the first patient cohort.

	Succeeded	Failed	Success rate (%)	*P* value[a]
Total (n = 71)	18	53	25	
Age, median (range)	73.6 (59–87)	69.5 (39–88)		*P* = 0.40
<60	1	11	8	
60–69	5	13	28	
70–79	8	15	35	
≥80	4	14	22	
Sex				*P* = 0.78
Male	10	32	24	
Female	8	21	28	
Stage				*P* = 0.92
IA	2	6	25	
IB	0	2	0	
IIA	5	9	36	
IIB	4	10	29	
IIIA	3	9	25	
IIIB	2	12	14	
IIIC	2	5	29	
IV	0	0	NA	
Tumor invasion				*P* = 0.73
T1	3	8	27	
T2	2	4	33	
T3	9	22	29	
T4	4	19	17	
LN metastasis				*P* = 0.55
N0	5	18	22	
N1	6	9	40	
N2	3	8	27	
N3a	2	13	13	
N3b	2	5	29	
Lauren's classification				*P* = 0.02
Intestinal	16	30	35	
Diffuse	2	23	8	
Location				*P* = 0.06
GE junction	2	0	100	
Fundus	4	6	40	
Corpus	5	25	17	
Antrum	7	22	24	
Metastasis at initial diagnosis				*P* = 1.00
Yes	2	5	29	
No	16	48	25	
Chemotherapy				*P* = 1.00
Before surgery	2	8	20	
No treatment	16	45	26	

[a]Fisher's exact test

Supplementary table 3: Success rates for spheroid establishment according to the clinicopathological characteristics of patients in the second patient cohort.

	Succeeded	Failed	Success rate (%)	*P* value[a]
Total (n = 33)	29	4	88	
Age, median (range)	79 (60-86)	76.5 (72-93)		*P* = 1.00
<60	0	0	NA	
60–69	5	0	100	
70–79	11	3	79	
≥80	13	1	93	
Sex				*P* = 1.00
Male	19	3	86	
Female	10	1	91	
Stage				*P* = 1.00
IA	6	0	100	
IB	1	0	100	
IIA	8	2	80	
IIB	6	0	100	
IIIA	1	1	50	
IIIB	5	1	83	
IIIC	2	0	100	
IV	0	0	NA	
Tumor invasion				*P* = 1.00
T1	8	0	100	
T2	7	1	88	
T3	8	3	73	
T4	6	0	100	
LN metastasis				*P* = 1.00
N0	12	2	86	
N1	4	0	100	
N2	6	0	100	
N3a	5	2	71	
N3b	2	0	100	
Lauren's classification				*P* = 1.00
Intestinal	23	3	88	
Diffuse	6	1	86	
Location				*P* = 1.00
GE junction	1	0	100	
Fundus	6	0	100	
Corpus	8	2	80	
Antrum	14	2	88	
Metastasis at initial diagnosis				*P* = 0.23
Yes	1	1	50	
No	28	3	90	
Chemotherapy				*P* = 0.33
Before surgery	2	1	67	
No treatment	27	3	90	

[a]Fisher's exact test

Supplementary table 4: Mutational status of 409 cancer-related genes in each gastric cancer stem cell (GC-SC) spheroid line in the first patient cohort detected using targeted next-generation sequencing.

Chrom	Position	Ref	Variant	Frequency	Type	Allele Name	Gene Symbol[a]	AAChange.refGene
HG1T								
chr3	187451403	T	C	41.2	SNV	---	BCL6	NM_001706:exon3:c.79A>G:p.S27G
chr4	62845473	A	C	63.6	SNV	---	ADGRL3	NM_015236:exon17:c.2794A>C:p.N932H
chr5	112163677	A	T	37.2	SNV	COSM18768	APC	NM_000038:exon13:c.1600A>T:p.K534X
chr5	112175303	C	T	62.8	SNV	COSM13129	APC	NM_000038:exon16:c.4012C>T:p.Q1338X
chr6	134492239	A	-	67.6	DEL	---	SGK1	NM_005627:exon10:c.960delT:p.I320fs
chr6	152476033	T	A	69.5	SNV	---	SYNE1	NM_033071:exon132:c.23910A>T:p.K7970N
chr6	166826287	C	T	35.4	SNV	---	RPS6KA2	NM_021135:exon21:c.2165G>A:p.R722H
chr7	151879573	T	C	30.8	SNV	---	KMT2C	NM_170606:exon36:c.5372A>G:p.Q1791R
chr9	134067664	C	A	45.8	SNV	---	NUP214	NM_005085:exon27:c.3644C>A:p.S1215X
chr11	3723971	G	C	51.2	SNV	---	NUP98	NM_016320:exon23:c.3234C>G:p.F1078L
chr12	56488301	A	G	33.9	SNV	---	ERBB3	NM_001982:exon15:c.1820A>G:p.Q607R
chr17	7577538	C	T	97.7	SNV	COSM10662	TP53	NM_000546:exon7:c.743G>A:p.R248Q
chr22	28195386	C	A	52.5	SNV	---	MN1	NM_002430:exon1:c.1146G>T:p.Q382H
HG2T[b]								
chr5	112175952	-	A	100.0	INS	COSM19695	APC	NM_000038:exon16:c.4662dupA:p.E1554fs
chr10	88649927	T	A	95.2	SNV	COSM9548662	BMPR1A	NM_004329:exon4:c.176T>A:p.L59X
chr17	7578223	C	T	100.0	SNV	COSM45995	TP53	NM_000546:exon6:c.626G>A:p.R209K
chr18	50278486	A	C	21.6	SNV	---	DCC	NM_005215:exon2:c.154A>C:p.M52L
HG3T[b]								
chr1	27023831	G	-	52.6	DEL	---	ARID1A	NM_006015:exon1:c.937delG:p.G313fs
chr1	27105617	C	T	52.9	SNV	---	ARID1A	NM_006015:exon20:c.5228C>T:p.T1743M
chr1	145532152	G	A	49.6	SNV	---	ITGA10	NM_003637:exon8:c.796G>A:p.E266K
chr1	147092593	T	C	49.2	SNV	---	BCL9	NM_004326:exon8:c.2632T>C:p.S878P
chr1	220808833	TC	-	50.1	DEL	---	MARK1	NM_018650:exon12:c.1238_1239del:p.I413fs
chr2	29451873	C	T	50.8	SNV	---	ALK	NM_004304:exon16:c.2692G>A:p.E898K
chr3	30691872	A	-	NA	DEL	---	TGFBR2	NM_003242:exon3;c.657Adel:p.K128fs
chr3	52442539	G	A	97.7	SNV	---	BAP1	NM_004656:exon4:c.206C>T:p.T69M
chr3	138461565	C	T	44.0	SNV	---	PIK3CB	NM_006219:exon3:c.456G>A:p.M152I
chr3	178952085	A	G	48.5	SNV	COSM94986	PIK3CA	NM_006218:exon21:c.3140A>G:p.H1047R
chr4	55152009	G	A	50.9	SNV	---	PDGFRA	NM_006206:exon18:c.2441G>A:p.C814Y
chr4	62936601	C	T	48.7	SNV	---	ADGRL3	NM_015236:exon25:c.4385C>T:p.P1462L
chr5	226052	C	T	50.3	SNV	---	SDHA	NM_004168:exon5:c.511C>T:p.R171C
chr5	176524337	G	T	49.5	SNV	---	FGFR4	NM_002011:exon17:c.2198G>T:p.R733M
chr6	31132590	C	T	57.5	SNV	---	POU5F1	NM_002701:exon5:c.871G>A:p.D291N
chr6	31138020	CTT	-	48.1	DEL	---	POU5F1	NM_002701:exon1:c.376_378del:p.126_126del
chr6	33287889	TCT	-	46.1	DEL	---	DAXX	NM_001350:exon5:c.1362_1364del:p.454_455del
chr6	41555186	C	-	56.0	DEL	---	FOXP4	NM_138457:exon7:c.805delC:p.P269fs
chr6	56327860	G	A	51.0	SNV	---	DST	NM_015548:exon82:c.15113C>T:p.P5038L
chr6	56462752	A	-	52.2	DEL	---	DST	NM_015548:exon28:c.4112delT:p.L1371fs
chr6	135518423	C	T	50.0	SNV	---	MYB	NM_001130173:exon10:c.1528C>T:p.R510C

chr7	2968323	G	-	58.8	DEL	---	CARD11	NM_032415:exon13:c.1663delC:p.R555fs
chr8	145737431	C	T	35.0	SNV	---	RECQL4	NM_004260:exon20:c.3256G>A:p.G1086R
chr8	145738671	T	C	29.3	SNV	---	RECQL4	NM_004260:exon15:c.2393A>G:p.Y798C
chr8	145739409	T	C	37.9	SNV	---	RECQL4	NM_004260:exon12:c.1961A>G:p.Q654R
chr9	120476084	-	A	29.4	INS	---	TLR4	NM_003266:exon4:c.1558dupA:p.S519fs
chr9	134039290	T	-	53.3	DEL	---	NUP214	NM_005085:exon20:c.2757delT:p.A919fs
chr9	135801117	C	A	45.8	SNV	---	TSC1	NM_000368:exon5:c.220G>T:p.D74Y
chr9	136901405	T	C	48.1	SNV	---	BRD3	NM_007371:exon10:c.1685A>G:p.D562G
chr10	76739022	A	G	51.1	SNV	---	KAT6B	NM_012330:exon10:c.2156A>G:p.Y719C
chr12	46246012	G	A	44.1	SNV	---	ARID2	NM_152641:exon15:c.4106G>A:p.G1369D
chr12	49431874	C	-	61.7	DEL	---	KMT2D	NM_003482:exon34:c.9265delG:p.V3089fs
chr13	110435906	C	T	47.8	SNV	---	IRS2	NM_003749:exon1:c.2495G>A:p.R832H
chr14	92471207	-	T	47.2	INS	---	TRIP11	NM_004239:exon11:c.3113dupA:p.K1038fs
chr15	40913546	AC	-	55.3	DEL	---	KNL1	NM_144508:exon10:c.1084_1085del:p.T362fs
chr16	23647028	T	-	52.0	DEL	---	PALB2	NM_024675:exon4:c.839delA:p.N280fs
chr16	50828253	T	C	49.9	SNV	---	CYLD	NM_015247:exon19:c.2600T>C:p.I867T
chr16	68857418	G	A	51.6	SNV	---	CDH1	NM_004360:exon13:c.2053G>A:p.V685M
chr17	29556478	G	T	49.2	SNV	---	NF1	NM_000267:exon21:c.2845G>T:p.G949X
chr17	78262019	-	C	28.2	INS	---	RNF213	NM_020954:exon4:c.667dupC:p.G222fs
chr17	78301694	A	G	49.9	SNV	---	RNF213	NM_001256071:exon19:c.3272A>G:p.K1091R
chr18	22807087	-	A	53.1	INS	---	ZNF521	NM_015461:exon4:c.795dupT:p.A266fs
chr18	50976892	C	-	78.7	DEL	---	DCC	NM_005215:exon23:c.3253delC:p.P1085fs
chr19	11141427	G	-	50.5	DEL	---	SMARCA4	NM_003072:exon25:c.3404delG:p.R1135fs
chr19	18870879	-	G	28.7	INS	---	CRTC1	NM_015321:exon8:c.727dupG:p.G243fs
chr19	45856398	G	A	48.0	SNV	---	ERCC2	NM_000400:exon19:c.1774C>T:p.R592C
chr19	52725449	A	G	37.3	SNV	---	PPP2R1A	NM_014225:exon13:c.1616A>G:p.N539S
chrX	44928908	C	T	99.2	SNV	---	KDM6A	NM_021140:exon17:c.2008C>T:p.Q670X
chrX	48121199	A	C	100.0	SNV	---	SSX1	NA (splicing)
chrX	66765779	G	-	100.0	DEL	---	AR	NM_000044:exon1:c.791delG:p.R264fs

HG4T

chr2	29543662	AT	GC	56.1	MNV	---	ALK	NM_004304:exon7:c.1500_1501GC
chr7	92734452	T	A	53.5	SNV	---	SAMD9	NM_017654:exon3:c.959A>T:p.Y320F
chr9	93627378	C	T	35.0	SNV	---	SYK	NM_003177:exon6:c.845C>T:p.A282V
chr10	43600607	C	A	61.2	SNV	COSM95173	RET	NM_020630:exon4:c.833delC:p.T278fs
chr11	47259484	G	A	29.0	SNV	---	DDB2	NM_000107:exon8:c.1120G>A:p.V374M
chr17	7577120	C	G	100.0	SNV	COSM43896	TP53	NM_000546:exon8:c.818G>C:p.R273P
chr22	41564594	T	C	100.0	SNV	---	EP300	NM_001429:exon24:c.4016T>C:p.M1339T

HG5T[b]

chr5	112174494	C	A	100.0	SNV	COSM4166493	APC	NM_000038:exon16:c.3203C>A:p.S1068X
chr8	48776032	T	A	21.9	SNV	---	PRKDC	NM_006904:exon42:c.5688A>T:p.E1893V
chr9	134019700	C	G	26.2	SNV	---	NUP214	NM_005085:exon12:c.1328C>G:p.A443G
chr11	102195701	TT	CA	56.5	MNV	---	BIRC3	NM_001165:exon2:c.461_462TT>CA:pF154S
chr17	7577117	A	G	100.0	SNV	COSM44393	TP53	NM_000546:exon8:c.821T>C:p.V274A
chrX	76939580	G	A	50.4	SNV	---	ATRX	NM_000489:exon9:c.1168C>T:p.R390C

HG6T

chr1	19018313	C	T	50.3	SNV	---	PAX7	NM_013945:exon5:c.646C>T:p.R216X

chr3	46490413	C	T	53.8	SNV	---	LTF	NM_002343:exon9:c.1153G>A:p.E385K
chr6	41564936	A	G	38.9	SNV	---	FOXP4	NM_138457:exon15:c.1642A>G:p.M548V
chr14	81609793	G	T	63.0	SNV	---	TSHR	NM_000369:exon10:c.1391G>T:p.G464V
chr17	7578212	G	A	99.2	SNV	COSM10654	TP53	NM_000546:exon6:c.637C>T:p.R213X
chr17	37881332	G	A	96.9	SNV	COSM14065	ERBB2	NM_004448:exon21:c.2524G>A:p.V842I
chrX	110366374	C	T	42.3	SNV	---	PAK3	NM_002578:exon5:c.43C>T:p.P15S

HG7T[b]

chr2	216272884	A	C	46.7	SNV	---	FN1	NM_002026:exon17:c.2465T>G:p.V822G
chr3	41266113	C	A	46.4	SNV	COSM5666	CTNNB1	NM_001904:exon3:c.110C>A:p.S37Y
chr6	117687341	T	C	72.0	SNV	---	ROS1	NM_002944:exon18:c.2710A>G:p.I904V
chr6	152540143	A	C	22.3	SNV	---	SYNE1	NM_033071:exon119:c.21826T>G:p.L7276V
chr7	2987388	G	A	78.9	SNV	COSM452940	CARD11	NM_032415:exon3:c.41C>T:p.T14M
chr7	106509517	C	G	28.0	SNV	---	PIK3CG	NM_002649:exon2:c.1511C>G:p.S504C
chr7	128851988	C	T	24.2	SNV	COSM5020286	SMO	NM_005631:exon12:c.2060C>T:p.P687L
chr9	21971007	CAGGTCCACGGG	-	100.0	DEL	---	CDKN2A	NM_000077:exon2:c.340_351del:p.114_117del
chr14	95569756	G	A	48.4	SNV	---	DICER1	NM_030621:exon23:c.3977C>T:p.A1326V
chr16	15931862	T	C	32.2	SNV	---	MYH11	NM_002474:exon2:c.248A>G:p.K83R
chr17				100.0			TP53	Large deletion[c]
chr19	18280013	C	A	45.2	SNV	---	PIK3R2	NM_005027:exon16:c.2096C>A:p.A699D
chr20	57480528	G	A	59.1	SNV	---	GNAS	NM_000516:exon6:c.523G>A:p.A175T
chrX	100608246	C	T	99.0	SNV	---	BTK	NM_000061:exon18:c.1844G>A:p.R615H

HG8T

No mutations in 409 cancer-related genes.

HG9T

chr5	7875383	C	A	30.6	SNV	---	MTRR	NM_002454:exon4:c.296C>A:p.S99X
chr8	71053424	T	A	74.0	SNV	---	NCOA2	NM_006540:exon14:c.3023A>T:p.N1008I
chr11	3752675	A	G	51.9	SNV	---	NUP98	NM_005387:exon14:c.1727T>C:p.F576S
chr15	41797675	G	A	94.5	SNV	---	LTK	NM_002344:exon14:c.1751C>T:p.T584I
chr17	7577126	T	A	95.0	SNV	COSM44469	TP53	NM_000546:exon8:c.812A>T:p.E271V
chr19	11143994	G	A	50.2	SNV	---	SMARCA4	NM_003072:exon26:c.3575G>A:p.R1192H
chr20	57430299	G	A	24.0	SNV	---	GNAS	NM_080425:exon1:c.1979G>A:p.R660H

HG10T

chr1	145532231	G	A	38.3	SNV	---	ITGA10	NM_003637:exon8:c.875G>A:p.C292Y
chr1	145537735	AG	-	38.7	DEL	---	ITGA10	NA (splicing)
chr1	179090821	A	G	48.8	SNV	---	ABL2	NM_005158:exon5:c.824T>C:p.M275T
chr1	220835187	G	T	46.9	SNV	---	MARK1	NM_018650:exon18:c.2067G>T:p.K689N
chr2	148672772	C	-	52.1	DEL	---	ACVR2A	NM_001616:exon5:c.541delC:p.P181fs
chr2	223161776	C	T	49.9	SNV	---	PAX3	NM_000438:exon2:c.242G>A:p.G81D
chr3	142280211	A	G	33.6	SNV	---	ATR	NM_001184:exon5:c.1223T>C:p.I408T
chr3	195593784	C	T	33.3	SNV	---	TNK2	NM_005781:exon14:c.3086G>A:p.G1029D
chr4	55151647	A	-	52.0	DEL	---	PDGFRA	NM_006206:exon17:c.2433delA:p.S811fs
chr4	153247175	-	T	49.8	INS	---	FBXW7	NM_018315:exon9:c.1387dupA:p.R463fs
chr5	180058748	G	-	43.1	DEL	---	FLT4	NM_002020:exon2:c.89delC:p.P30fs
chr6	41555186	C	-	44.1	DEL	---	FOXP4	NM_138457:exon7:c.805delC:p.P269fs

chr6	51612648	G	A	50.4	SNV	---	PKHD1	NM_170724:exon58:c.9766C>T:p.P3256S
chr6	70048837	C	T	49.0	SNV	---	ADGRB3	NM_001704:exon25:c.3218C>T:p.T1073M
chr6	106547205	A	G	38.8	SNV	---	PRDM1	NM_001198:exon4:c.442A>G:p.I148V
chr6	135507123	C	T	52.3	SNV	---	MYB	NM_005375:exon2:c.106C>T:p.R36C
chr6	152472716	T	A	48.6	SNV	---	SYNE1	NM_033071:exon134:c.24209A>T:p.D8070V
chr8	41791555	C	T	29.8	SNV	---	KAT6A	NM_006766:exon17:c.4183G>A:p.D1395N
chr8	48689466	G	-	22.1	DEL	---	PRKDC	NM_006904:exon85:c.12127delC:p.P4040fs
chr8	92983013	G	A	34.0	SNV	COSM33136	RUNX1T1	NM_004349:exon10:c.1331C>T:p.A444V
chr8	92983068	C	T	34.8	SNV	---	RUNX1T1	NM_004349:exon10:c.1276G>A:p.V426I
chr9	133760106	C	T	49.4	SNV	---	ABL1	NM_005157:exon11:c.2429C>T:p.P810L
chr12	46215214	T	-	26.5	DEL	---	ARID2	NM_152641:exon6:c.649delT:p.F217fs
chr12	46243853	T	-	45.6	DEL	---	ARID2	NM_152641:exon15:c.1947delT:p.H649fs
chr12	49430935	GCT	-	34.3	DEL	---	KMT2D	NM_003482:exon34:c.10202_10204del:p.3401_3402del
chr12	49443503	G	A	49.9	SNV	---	KMT2D	NM_003482:exon11:c.3868C>T:p.R1290W
chr12	49444842	G	T	51.9	SNV	---	KMT2D	NM_003482:exon10:c.2624C>A:p.P875H
chr12	121432117	GC	-	43.5	DEL	---	HNF1A	NM_000545:exon4:c.864_865del:p.G288fs
chr12	121432118	CC	-	56.5	DEL	---	HNF1A	NM_000545:exon4:c.865_866del:p.P289fs
chr13	110435136	C	G	43.2	SNV	---	IRS2	NM_003749:exon1:c.3265G>C:p.A1089P
chr14	102551189	CTT	-	48.4	DEL	---	HSP90AA1	NM_005348:exon5:c.806_808del:p.269_270del
chr15	88726662	G	T	47.5	SNV	---	NTRK3	NM_002530:exon5:c.382C>A:p.H128N
chr17	8110652	C	T	49.3	SNV	---	AURKB	NM_001313955:exon4:c.17G>A:p.G6D
chr17	41607297	G	A	49.1	SNV	---	ETV4	NM_001986:exon10:c.910C>T:p.R304X
chr17	75478295	C	T	52.8	SNV	---	SEPT9	NM_006640:exon3:c.737C>T:p.A246V
chr18	59195372	A	T	100.0	SNV	---	CDH20	NM_031891:exon7:c.1190A>T:p.E397V
chr19	11144149	C	T	54.2	SNV	---	SMARCA4	NM_003072:exon26:c.3730C>T:p.R1244C
chr20	31022281	C	A	52.5	SNV	---	ASXL1	NM_015338:exon12:c.1766C>A:p.P589H
chrX	41075161	G	A	46.3	SNV	---	USP9X	NM_001039590:exon35:c.5341G>A:p.V1781I
chrX	153762700	C	T	44.5	SNV	---	G6PD	NM_000402:exon6:c.587G>A:p.R196H

HG11T

chr1	45795081	G	A	68.7	SNV	---	MUTYH	NM_012222:exon16:c.1538C>T:p.P513L
chr2	24952578	T	C	27.4	SNV	---	NCOA1	NM_003743:exon15:c.3095T>C:p.F1032S
chr4	62936411	C	A	47.2	SNV	---	ADGRL3	NM_015236:exon25:c.4195C>A:p.Q1399K
chr15	66729181	A	G	62.2	SNV	---	MAP2K1	NM_002755:exon3:c.389A>G:p.Y130C
chr17	7578263	G	A	100.0	SNV	COSM10705	TP53	NM_000546:exon6:c.586C>T:p.R196X
chr17	37880257	C	G	100.0	SNV	COSM51317	ERBB2	NM_004448:exon19:c.2301C>G:p.I767M

HG12T

chr1	162725039	G	A	40.8	SNV	---	DDR2	NM_006182:exon6:c.511G>A:p.D171N
chr2	141459833	C	T	49.0	SNV	---	LRP1B	NM_018557:exon39:c.6179G>A:p.R2060H
chr6	152129391	C	T	56.5	SNV	---	ESR1	NM_000125:exon1:c.344C>T:p.P115L
chr6	152129451	A	G	41.8	SNV	---	ESR1	NM_000125:exon1:c.404A>G:p.E135G
chr6	152472810	G	A	47.2	SNV	---	SYNE1	NM_033071:exon134:c.24115C>T:p.R8039C
chr6	152532711	C	T	46.0	SNV	---	SYNE1	NM_033071:exon123:c.22294G>A:p.E7432K
chr7	2946337	C	T	59.7	SNV	---	CARD11	NM_032415:exon25:c.3400G>A:p.V1134I
chr16	65005506	T	G	24.2	SNV	---	CDH11	NM_001797:exon11:c.1618A>C:p.N540H
chr16	66426109	G	A	53.8	SNV	---	CDH5	NM_001795:exon7:c.1040G>A:p.R347Q
chr16	68863616	C	G	51.4	SNV	---	CDH1	NM_004360:exon15:c.2355C>G:p.N785K
chr17	37868208	C	A	58.1	SNV	---	ERBB2	NM_004448:exon8:c.929C>A:p.S310Y

chr19	18279669	G	A	57.0	SNV	---	PIK3R2	NM_005027:exon15:c.1942G>A:p.E648K

HG13T

chr1	162724541	C	T	44.1	SNV	---	DDR2	NM_006182:exon5:c.313C>T:p.R105C
chr1	185069410	G	A	40.2	SNV	---	RNF2	NM_007212:exon7:c.988G>A:p.A330T
chr1	241680541	C	T	44.0	SNV	---	FH	NM_000143:exon2:c.208G>A:p.A70T
chr2	141294155	T	A	51.5	SNV	---	LRP1B	NM_018557:exon46:c.7637A>T:p.Y2546F
chr2	148683686	A	-	57.7	DEL	---	ACVR2A	NM_001616:exon10:c.1304delA:p.K435fs
chr2	216292965	G	A	57.6	SNV	---	FN1	NM_054034:exon6:c.782C>T:p.T261I
chr2	223163270	C	T	31.6	SNV	---	PAX3	NM_000438:exon1:c.65G>A:p.R22H
chr3	37090443	T	C	89.9	SNV	---	MLH1	NM_000249:exon18:c.2038T>C:p.C680R
chr3	187447511	G	A	26.1	SNV	---	BCL6	NM_001706:exon5:c.682C>T:p.R228W
chr5	180047947	G	A	45.7	SNV	---	FLT4	NM_002020:exon15:c.2228C>T:p.A743V
chr6	56476324	A	-	58.3	DEL	---	DST	NM_015548:exon24:c.3518delT:p.L1173fs
chr6	117609728	C	T	52.2	SNV	---	ROS1	NM_002944:exon43:c.6971G>A:p.C2324Y
chr7	116409799	C	T	47.8	SNV	---	MET	NM_000245:exon12:c.2684C>T:p.T895M
chr8	113267554	A	T	49.8	SNV	---	CSMD3	NM_052900:exon60:c.9458T>A:p.I3153K
chr9	136913503	G	A	78.4	SNV	---	BRD3	NM_007371:exon6:c.788C>T:p.S263L
chr10	89693007	A	-	65.2	DEL	COSM5847	PTEN	NM_000314:exon5:c.487delA:p.K163fs
chr10	89725051	T	G	55.7	SNV	---	PTEN	NM_000314:exon9:c.1034T>G:p.L345R
chr11	32456771	C	T	53.4	SNV	---	WT1	NM_000378:exon1:c.121G>A:p.A41T
chr13	110436710	G	A	57.4	SNV	---	IRS2	NM_003749:exon1:c.1691C>T:p.A564V
chr14	99642275	G	A	44.4	SNV	---	BCL11B	NM_022898:exon3:c.685C>T:p.R229W
chr14	99642286	C	-	44.4	DEL	---	BCL11B	NM_022898:exon3:c.674delG:p.G225fs
chr17	7577121	G	A	92.8	SNV	COSM99933	TP53	NM_000546:exon8:c.817C>T:p.R273C
chr17	29661945	C	T	64.1	SNV	COSM30766	NF1	NM_000267:exon39:c.5839C>T:p.R1947X
chr18	45394825	A	-	26.4	DEL	---	SMAD2	NM_005901:exon5:c.524delT:p.L175fs
chr19	18278020	G	A	48.8	SNV	---	PIK3R2	NM_005027:exon13:c.1640G>A:p.R547Q
chr20	57484420	C	T	55.6	SNV	COSM123397	GNAS	NM_000516:exon8:c.601C>T:p.R201C
chrX	48544188	G	T	45.2	SNV	---	WAS	NM_000377:exon4:c.426G>T:p.Q142H
chrX	63411537	G	A	21.0	SNV	---	AMER1	NM_152424:exon2:c.1630C>T:p.P544S
chrX	70627470	C	T	44.2	SNV	---	TAF1	NM_004606:exon27:c.4214C>T:p.T1405M

HG14T

chr2	24914529	G	T	48.7	SNV	---	NCOA1	NM_003743:exon7:c.712G>T:p.D238Y
chr3	30713544	AGA	-	51.8	DEL	---	TGFBR2	NM_003242:exon4:c.869_871del:p.290_291del
chr3	52442567	G	A	98.7	SNV	---	BAP1	NM_004656:exon4:c.178C>T:p.R60X
chr3	178936091	G	A	51.0	SNV	COSM125370	PIK3CA	NM_006218:exon10:c.1633G>A:p.E545K
chr16	68844179	A	G	98.4	SNV	---	CDH1	NM_004360:exon6:c.767A>G:p.N256S
chr17	7578496	A	C	97.3	SNV	COSM45351	TP53	NM_000546:exon5:c.434T>G:p.L145R
chrX	70674025	G	C	37.3	SNV	---	TAF1	NM_004606:exon33:c.4819G>C:p.E1607Q

HG15T

chr2	219562333	C	T	59.4	SNV	---	STK36	NM_015690:exon24:c.2909C>T:p.A970V
chr3	89259092	A	C	28.0	SNV	---	EPHA3	NM_005233:exon3:c.236A>C:p.N79T
chr5	112170745	C	-	100.0	DEL	---	APC	NM_000038:exon15:c.1841delC:p.A614fs
chr6	152675840	C	T	75.5	SNV	---	SYNE1	NM_182961:exon67:c.10880G>A:p.R3627H
chr11	71729920	C	T	62.1	SNV	---	NUMA1	NM_006185:exon10:c.691G>A:p.D231N
chr11	106810667	G	T	63.0	SNV	---	GUCY1A2	NM_000855:exon4:c.725C>A:p.P242H

chr12	25398285	C	T	38.2	SNV	COSM517	KRAS	NM_004985:exon2:c.34G>A:p.G12S
chr16	14028150	G	C	35.3	SNV	---	ERCC4	NM_005236:exon7:c.1204G>C:p.G402R
chr17	7577094	G	A	100.0	SNV	COSM10704	TP53	NM_000546:exon8:c.844C>T:p.R282W
chr17	11958269	C	T	46.8	SNV	---	MAP2K4	NM_003010:exon2:c.179C>T:p.T60I
chr18	48573628	G	T	54.9	SNV	COSM7410653	SMAD4	NM_005359:exon2:c.212G>T:p.C71F
chrX	110391010	A	C	45.6	SNV	---	PAK3	NM_002578:exon7:c.322A>C:p.T108P

HG16T

chr3	3209379	G	A	50.8	SNV	---	CRBN	NM_016302:exon5:c.626C>T:p.P209L
chr5	112176017	G	T	100.0	SNV	COSM236691	APC	NM_000038:exon16:c.4726G>T:p.E1576X
chr6	152599391	T	A	50.6	SNV	---	SYNE1	NM_033071:exon97:c.18193A>T:p.K6065X,
chr8	71036145	C	G	54.7	SNV	---	NCOA2	NM_006540:exon21:c.4267G>C:p.G1423R
chr8	113651126	A	C	51.3	SNV	---	CSMD3	NM_052900:exon20:c.3013T>G:p.F1005V
chr8	37697642	G	A	49.2	SNV	---	ADGRA2	NM_032777:exon17:c.2515G>A:p.G839S
chr10	104159195	CA	TG	42.2	MNV	---	NFKB2	NM_002502:exon13:c.1268_1269TG
chr11	106680767	T	G	48.9	SNV	---	GUCY1A2	NM_000855:exon5:c.1644A>C:p.E548D
chr17	5424974	A	G	100.0	SNV	---	NLRP1	NM_033004:exon13:c.3653T>C:p.L1218P
chr17	7578449	C	A	100.0	SNV	COSM43549	TP53	NM_000546:exon5:c.481G>T:p.A161S
chr18	59217341	A	C	30.9	SNV	---	CDH20	NM_031891:exon11:c.1779A>C:p.Q593H
chr20	40980892	T	G	50.4	SNV	---	PTPRT	NM_007050:exon10:c.1594A>C:p.S532R
chr21	39817504	T	G	91.1	SNV	---	ERG	NM_004449:exon4:c.80A>C:p.E27A

HG17T

chr1	47691173	C	T	73.3	SNV	---	TAL1	NM_003189:exon4:c.388G>A:p.A130T
chr1	145537512	G	A	50.1	SNV	---	ITGA10	NM_003637:exon20:c.2522G>A:p.S841N
chr1	237058733	G	A	50.3	SNV	---	MTR	NM_000254:exon31:c.3481G>A:p.A1161T
chr2	5833692	C	T	56.5	SNV	---	SOX11	NM_003108:exon1:c.839C>T:p.T280M
chr2	140990847	G	A	53.1	SNV	---	LRP1B	NM_018557:exon91:c.13708C>T:p.Q4570X
chr2	141114024	T	A	47.3	SNV	---	LRP1B	NM_018557:exon75:c.11417A>T:p.E3806V
chr2	141625795	G	A	44.0	SNV	---	LRP1B	NM_018557:exon26:c.4207C>T:p.R1403C
chr2	219544700	G	A	51.5	SNV	---	STK36	NM_015690:exon9:c.1033G>A:p.G345R
chr3	138664876	G	A	61.2	SNV	---	FOXL2	NM_023067:exon1:c.689C>T:p.A230V
chr4	1807388	C	T	47.0	SNV	---	FGFR3	NM_000142:exon12:c.1637C>T:p.T546M
chr4	1962801	G	A	49.1	SNV	---	NSD2	NM_133330:exon20:c.3295G>A:p.E1099K
chr4	1978254	C	T	46.4	SNV	---	NSD2	NM_133330:exon23:c.3674C>T:p.T1225M
chr4	55138644	C	T	54.2	SNV	---	PDGFRA	NM_006206:exon9:c.1321C>T:p.P441S
chr4	55970882	C	T	49.7	SNV	---	KDR	NM_002253:exon13:c.1915G>A:p.D639N
chr4	87968244	G	A	44.9	SNV	---	AFF1	NM_005935:exon3:c.536G>A:p.R179Q
chr5	176524292	G	T	53.3	SNV	---	FGFR4	NA (splicing)
chr6	51612675	C	T	52.0	SNV	---	PKHD1	NM_138694:exon58:c.9739G>A:p.V3247I
chr6	69348958	C	T	37.5	SNV	---	ADGRB3	NM_001704:exon3:c.391C>T:p.R131C
chr6	152461296	C	A	50.5	SNV	---	SYNE1	NM_033071:exon140:c.25103G>T:p.G8368V
chr6	152539487	C	T	48.7	SNV	---	SYNE1	NM_033071:exon120:c.21883G>A:p.A7295T
chr7	13971195	G	A	48.2	SNV	---	ETV1	NM_004956:exon9:c.734C>T:p.A245V
chr7	98547355	C	T	46.4	SNV	---	TRRAP	NM_003496:exon35:c.4951C>T:p.R1651C
chr7	98608684	G	A	50.4	SNV	---	TRRAP	NM_003496:exon69:c.10819G>A:p.D3607N
chr7	126544156	T	-	99.3	DEL	---	GRM8	NM_000845:exon4:c.887delA:p.K296fs
chr7	128845518	C	T	49.2	SNV	---	SMO	NM_005631:exon4:c.815C>T:p.A272V
chr7	152055732	C	G	100.0	SNV	---	KMT2C	NM_170606:exon2:c.190G>C:p.E64Q

chr8	145739598	C	T	31.1	SNV	---	RECQL4	NM_004260:exon11:c.1853G>A:p.R618Q
chr10	76789461	G	A	53.7	SNV	---	KAT6B	NM_012330:exon18:c.4879G>A:p.A1627T
chr10	104160958	ACG	-	53.6	DEL	---	NFKB2	NM_002502:exon19:c.2093_2095del:p.698_699del
chr10	104160962	G	T	53.4	SNV	---	NFKB2	NM_002502:exon19:c.2097G>T:p.E699D
chr11	32456494	G	A	69.1	SNV	---	WT1	NM_024426:exon1:c.398C>T:p.P133L
chr11	118377154	G	A	53.0	SNV	---	KMT2A	NM_005933:exon27:c.10538G>A:p.G3513E
chr12	46123699	A	G	51.4	SNV	---	ARID2	NM_152641:exon1:c.80A>G:p.H27R
chr12	49434492	G	-	55.1	DEL	---	KMT2D	NM_003482:exon31:c.7061delC:p.P2354fs
chr12	56481660	C	T	46.8	SNV	---	ERBB3	NM_001982:exon6:c.695C>T:p.A232V
chr12	121432115	G	-	55.3	DEL	---	HNF1A	NM_000545:exon4:c.862delG:p.G288fs
chr13	28959144	C	T	42.6	SNV	---	FLT1	NM_002019:exon14:c.1994G>A:p.R665Q
chr13	110435129	G	A	64.2	SNV	---	IRS2	NM_003749:exon1:c.3272C>T:p.P1091L
chr14	23776992	T	G	51.6	SNV	---	BCL2L2	NM_004050:exon3:c.16T>G:p.S6A
chr14	99642359	C	-	100.0	DEL	---	BCL11B	NM_022898:exon3:c.601delG:p.E201fs
chr15	88420264	G	A	47.5	SNV	---	NTRK3	NM_002530:exon19:c.2380C>T:p.Q794X
chr15	91295095	A	G	55.5	SNV	---	BLM	NM_000057:exon4:c.878A>G:p.D293G
chr16	3807902	G	A	50.1	SNV	---	CREBBP	NM_004380:exon18:c.3517C>T:p.R1173X
chr17	8110651	G	A	52.5	SNV	---	AURKB	NM_004217:exon5:c.241C>T:p.R81C
chr17	45360843	G	A	51.3	SNV	---	ITGB3	NM_000212:exon3:c.289G>A:p.D97N
chr19	42795811	C	T	44.3	SNV	---	CIC	NM_015125:exon11:c.2800C>T:p.R934W
chr19	57744888	G	T	46.7	SNV	---	AURKC	NM_003160:exon5:c.394G>T:p.D132Y
chr20	31017181	G	A	50.0	SNV	---	ASXL1	NM_015338:exon6:c.512G>A:p.R171Q
chr20	31017747	-	CAG	52.3	INS	---	ASXL1	NM_015338:exon7:c.608_609insCAG:p.S203delinsSS
chr20	31019407	C	T	49.9	SNV	---	ASXL1	NM_015338:exon9:c.904C>T:p.R302C
chr20	57415336	C	T	65.0	SNV	---	GNAS	NM_016592:exon1:c.175C>T:p.Q59X
chr20	57415354	C	T	65.1	SNV	---	GNAS	NM_016592:exon1:c.193C>T:p.L65F
chr20	57429959	C	T	46.3	SNV	---	GNAS	NM_080425:exon1:c.1639C>T:p.R547C
chr22	33198077	C	-	52.1	DEL	---	TIMP3	NM_000362:exon1:c.90delC:p.H30fs

HG18T

chr3	3214610	C	A	45.8	SNV	---	CRBN	NA (splicing)
chr3	128204594	G	A	50.9	SNV	---	GATA2	NM_032638:exon3:c.847C>T:p.R283C
chr3	134851696	C	T	51.0	SNV	---	EPHB1	NM_004441:exon5:c.1102C>T:p.R368W
chr8	114111160	A	G	28.5	SNV	---	CSMD3	NM_052900:exon5:c.742T>C:p.S248P
chr11	94194148	-	A	61.6	INS	---	MRE11	NM_005590:exon12:c.1280dupT:p.L427fs
chr17	7578418	T	C	100.0	SNV	COSM44732	TP53	NM_000546:exon5:c.512A>G:p.E171G
chr21	46313417	C	T	47.6	SNV	---	ITGB2	NM_000211:exon10:c.1126G>A:p.D376N

Abbreviations: SNV, single nucleotide variant; MNV, multiple nucleotide variant; INS, insertion; DEL, deletion.

[a]The list of 409 genes is available at http://assets.thermofisher.com/TFS-Assets/CSD/Reference-Materials/ion-ampliseq-cancer-panel-gene-list.pdf.

[b]The cancer-specific mutations were detected referring to the profiles of matched normal DNA.

[c]The gene deletion was detected with Integrative Genomics Viewer.

Supplementary table 5: Mutational status of 409 cancer-related genes in 25 gastric cancer stem cell (GC-SC) spheroid lines in the second patient cohort detected using RNA sequencing (RNA-seq).

Chrom	Position	Ref	Variant	Frequency	Type	Allele Name	Gene Symbol[a]	AAChange.refGene
HG19T								
chr9	134053745	G	A	36.4	SNV	---	NUP214	NM_005085:exon24:c.3367G>A:p.V1123I
chr17	7577120	C	T	100.0	SNV	COSM10660	TP53	NM_001126115:exon4:c.422G>A:p.R141H
HG20T								
chr6	56566690	C	T	54.5	SNV	---	DST	NM_183380:exon4:c.317G>A:p.R106H
chr17	7577094	G	A	100.0	SNV	COSM10704	TP53	NM_000546:exon8:c.844C>T:p.R282W
chr19	11170854	A	C	100.0	SNV	---	SMARCA4	NM_003072:exon34:c.4902A>C:p.E1634D
HG21T								
chr3	30732970	G	A	65.2	SNV	COSM33076	TGFBR2	NM_003242:exon7:c.1583G>A:p.R528H
chr17	37880261	G	T	97.6	SNV	COSM1251412	ERBB2	NM_004448:exon19:c.2305G>T:p.D769Y
chr17				100.0		---	TP53	Splicing[b]
chr19	11101959	AGA	-	47.2	DEL	COSM30583	SMARCA4	NM_003072:exon8:c.1379_1381del:p.460_461del
HG22T								
No detectable mutations in 409 cancer-related genes.								
HG23T								
chr1	27106320	-	G	33.3	INS	COSM6916114	ARID1A	NM_006015:exon20:c.5932dupG:p.L1977fs
HG24T								
No detectable mutations in 409 cancer-related genes.								
HG25T								
chr13	48934188	T	C	60.0	SNV	---	RB1	NM_000321:exon7:c.643T>C:p.S215P
chr16	3828111	G	A	30.4	SNV	COSM7347140	CREBBP	NM_004380:exon10:c.2014C>T:p.R672C
chr17	37682291	C	T	50.0	SNV	---	CDK12	NM_015083:exon13:c.3482C>T:p.T1161M
HG26T								
chr8	57079350	T	C	55.0	SNV	---	PLAG1	NM_002655:exon5:c.955A>G:p.I319V
chr20	39795470	G	A	47.0	SNV	COSM3291377	PLCG1	NM_002660:exon19:c.2272G>A:p.E758K
HG28T								
chr17	7577100	T	C	100.0	SNV	COSM11123	TP53	NM_000546:exon8:c.838A>G:p.R280G
HG29T								
chr1	27106804	C	-	42.1	DEL	---	ARID1A	NM_006015:exon20:c.6415delC:p.P2139fs
chr2	148683686	A	-	54.2	DEL	---	ACVR2A	NM_001616:exon10:c.1303delA:p.K435fs
chr3	30691872	AA	-	100.0	DEL	COSM5989666	TGFBR2	NM_001024847:exon4:c.449_450del:p.E150fs
chr3	30691873	-	A	100.0	INS	---	TGFBR2	NM_001024847:exon4:c.450dupA:p.E150fs
chr3	66023896	C		37.5	DEL	---	MAGI1	NM_004742:exon1:c.88delG:p.V30X

chr3	69928320	C	T	62.5	SNV	---	MITF	NM_006722:exon2:c.137C>T:p.P46L
chr3	187447663	C	T	55.8	SNV	---	BCL6	NM_001706:exon5:c.530G>A:p.S177N
chr3	195595423	C	A	41.1	SNV	---	TNK2	NM_005781:exon12:c.1701G>T:p.E567D
chr3	195615342	A	G	36.7	SNV	---	TNK2	NM_005781:exon2:c.118T>C:p.Y40H
chr5	138223183	G	A	36.2	SNV	COSM6369106	CTNNA1	NM_001903:exon9:c.1148G>A:p.R383H
chr5	176722087	C	-	35.7	DEL	---	NSD1	NM_022455:exon23:c.7718delC:p.S2573fs
chr6	52876605	G	A	40.9	SNV	---	ICK	NM_014920:exon11:c.1454C>T:p.A485V
chr6	56434717	T	-	41.9	DEL	---	DST	NM_015548:exon35:c.5946delA:p.K1982fs
chr6	56600064	T	C	33.3	SNV	---	DST	NM_183380:exon2:c.115A>G:p.K39E
chr7	116395528	T	A	48.7	SNV	---	MET	NM_000245:exon6:c.1821T>A:p.N607K
chr9	120475384	TTC	-	42.1	DEL	---	TLR4	NM_003266:exon4:c.858_860del:p.286_287del
chr9	133759541	C	T	47.5	SNV	---	ABL1	NM_005157:exon11:c.1864C>T:p.R622W
chr9	133759623	C	-	31.6	DEL	---	ABL1	NM_005157:exon11:c.1946delC:p.T649fs
chr9	133760108	C	T	25.9	SNV	---	ABL1	NM_005157:exon11:c.2431C>T:p.P811S
chr10	76735496	G	C	56.3	SNV	---	KAT6B	NM_012330:exon8:c.1401G>C:p.K467N
chr10	76788342	C	T	36.5	SNV	COSM257480	KAT6B	NM_012330:exon18:c.3760C>T:p.R1254C
chr11	69456196	G	A	48.3	SNV	---	CCND1	NM_053056:exon1:c.115G>A:p.A39T
chr11	95825682	C	T	40.0	SNV	---	MAML2	NM_032427:exon2:c.1513G>A:p.G505S
chr12	25398284	C	T	53.3	SNV	COSM521	KRAS	NM_004985:exon2:c.35G>A:p.G12D
chr12	132510328	C	T	34.8	SNV	---	EP400	NM_015409:exon25:c.4993C>T:p.P1665S
chr15	74315557	G	A	34.1	SNV	COSM1937940	PML	NM_002675:exon3:c.991G>A:p.A331T
chr16	14029219	G	A	46.2	SNV	COSM8194527	ERCC4	NM_005236:exon8:c.1430G>A:p.R477Q
chr17	5436192	G	-	28.6	DEL	---	NLRP1	NM_014922:exon11:c.3246delC:p.P1082fs
chr17	12043184	A	G	27.0	SNV	---	MAP2K4	NM_003010:exon10:c.1069A>G:p.K357E
chr17	75484906	G	A	38.0	SNV	---	SEPT9	NM_006640:exon6:c.1168G>A:p.V390I
chr19	18870855	C	A	40.5	SNV	---	CRTC1	NM_015321:exon8:c.703C>A:p.L235M
chr19	45855781	T	C	28.9	SNV	COSM1630983	ERCC2	NM_000400:exon21:c.2029A>G:p.M677V
chr20	54958077	T	C	26.5	SNV	---	AURKA	NM_003600:exon5:c.530A>G:p.Q177R
chr20	54961519	G	T	38.3	SNV	COSM6274846	AURKA	NM_003600:exon3:c.113C>A:p.P38H
chrX	44732910	C	-	41.2	DEL	---	KDM6A	NM_021140:exon1:c.113delC:p.S38fs

HG32T

Chr1	2493196	C	G	51.1	SNV	---	TNFRSF14	NM_003820:exon6:c.636C>G:p.I212M
Chr2	148672848	T	C	58.1	SNV	---	ACVR2A	NM_001616:exon5:c.617T>C:p.V206A
Chr3	142188286	T	G	32.4	SNV	---	ATR	NM_001184:exon38:c.6445A>C:p.I2149L
Chr20	36030983	C	T	32.6	SNV	COSM4430704	SRC	NM_005417:exon12:c.1262C>T:p.A421V

HG33T

chr3	10084304	T	C	28.6	SNV	---	FANCD2	NM_033084:exon11:c.845T>C:p.I282T
chr6	56434742	G	A	33.3	SNV	---	DST	NM_015548:exon35:c.5921C>T:p.S1974L
chr6	56434780	C	A	100.0	SNV	---	DST	NM_015548:exon35:c.5883G>T:p.Q1961H
chr6	56505257	A	G	28.6	SNV	---	DST	NM_015548:exon4:c.563T>C:p.L188S
chr11	108117816	G	A	40.0	SNV	---	ATM	NM_000051:exon8:c.1027G>A:p.E343K
chr15	99251312	T	C	50.0	SNV	---	IGF1R	NM_000875:exon2:c.616T>C:p.W206R
chr17	7576873	C	A	100.0	SNV	COSM307331	TP53	NM_000546:exon9:c.973G>T:p.G325X
chr22	23652547	G	A	35.0	SNV	---	BCR	NM_004327:exon18:c.3109G>A:p.E1037K

HG34T

chr5	112173917	C	T	50.0	SNV	COSM18852	APC	NM_000038:exon16:c.2626C>T:p.R876X

chr5	112175639	C	T	58.3	SNV	COSM13127	APC	NM_000038:exon16:c.4348C>T:p.R1450X
chr11	71726490	C	T	47.8	SNV	COSM9833905	NUMA1	NM_006185:exon15:c.2059G>A:p.A687T
chr12	46230707	C	T	66.7	SNV	COSM6955940	ARID2	NM_152641:exon8:c.956C>T:p.S319F
HG35T								
chr1	27106861	C	T	56.3	SNV	COSM51432	ARID1A	NM_006015:exon20:c.6472C>T:p.R2158X
chr5	112175799	C	A	100.0	SNV	COSM5732639	APC	NM_000038:exon16:c.4508C>A:p.S1503X
chr10	49612963	A	C	50.0	SNV	---	MAPK8	NM_139046:exon5:c.191A>C:p.Q64P
chr12	56489535	G	A	54.5	SNV	COSM1677075	ERBB3	NM_001982:exon17:c.2000G>A:p.R667H
chr17				100.0		---	TP53	Splicing[b]
HG36T								
chr16	50830391	A	G	48.9	SNV	---	CYLD	NM_015247:exon20:c.2843A>G:p.Q948R
chr17	29509642	G	T	30.4	SNV	COSM3179569	NF1	NM_000267:exon8:c.847G>T:p.D283Y
HG37T								
chr2	47690192	T	C	52.4	SNV	---	MSH2	NM_000251:exon9:c.1409T>C:p.V470A
chr7	116422120	G	T	37.1	SNV	---	MET	NM_000245:exon18:c.3601G>T:p.V1201F
chr17	7577547	C	A	100.0	SNV	COSM11196	TP53	NM_000546:exon7:c.734G>T:p.G245V
HG38T								
chr10	102891485	G	A	100.0	SNV	---	TLX1	NM_005521:exon1:c.187G>A:p.A63T
chr14	92482072	C	T	47.6	SNV	COSM6279187	TRIP11	NM_004239:exon6:c.791G>A:p.R264Q
chr17	7577574	T	C	100.0	SNV	COSM10731	TP53	NM_000546:exon7:c.707A>G:p.Y236C
HG39T								
chr15	90633765	A	G	48.0	SNV	---	IDH2	NM_002168:exon3:c.319T>C:p.Y107H
chr17	48264477	G	A	51.9	SNV	---	COL1A1	NM_000088:exon47:c.3430C>T:p.P1144S
HG40T								
chr1	226564855	G	A	60.0	SNV	COSM1219296	PARP1	NM_001618:exon13:c.1895C>T:p.T632M
chr6	160468835	C	A	39.6	SNV	---	IGF2R	NM_000876:exon17:c.2241C>A:p.N747K
chr22	41554449	G	A	40.0	SNV	---	EP300	NM_001429:exon19:c.3535G>A:p.G1179S
HG42T								
chr1	27087503	C	T	100.0	SNV	COSM184236	ARID1A	NM_006015:exon5:c.2077C>T:p.R693X
chr3	178936091	G	A	42.9	SNV	COSM763	PIK3CA	NM_006218:exon10:c.1633G>A:p.E545K
chr5	112176008	G	T	43.8	SNV	COSM4167225	APC	NM_000038:exon16:c.4717G>T:p.E1573X
chr22	23655131	C	T	32.8	SNV	---	BCR	NM_004327:exon20:c.3380C>T:p.T1127M
chr22	41546045	C	T	56.5	SNV	---	EP300	NM_001429:exon14:c.2660C>T:p.T887I
HG43T								
chr7	2956956	G	C	41.3	SNV	---	CARD11	NM_032415:exon20:c.2671C>G:p.R891G
HG44T								
chr6	51890782	T	C	50.0	SNV	---	PKHD1	NM_170724:exon32:c.3826A>G:p.R1276G
chr6	152461248	T	C	33.3	SNV	---	SYNE1	NM_033071:exon140:c.25151A>G:p.E8384G
chr7	2959046	C	G	29.3	SNV	COSM452935	CARD11	NM_032415:exon18:c.2470G>C:p.D824H
chr9	22006138	G	A	100.0	SNV	COSM6983462	CDKN2B	NM_004936:exon2:c.265C>T:p.R89W

chr15	91292605	C	T	25.0	SNV	---	BLM	NM_000057:exon3:c.107C>T:p.T36I
HG45T								
chr7	2977555	G	A	31.3	SNV	COSM3027901	CARD11	NM_032415:exon8:c.1129C>T:p.R377W
HG46T								
chr11	64572285	G	A	68.8	SNV	COSM8474098	MEN1	NM_000244:exon10:c.1369C>T:p.R457W
chr17	7579311	C	T	100.0	SNV	---	TP53	Splicing[b]
HG47T								
chr1	179077046	T	A	50.0	SNV	---	ABL2	NM_007314:exon12:c.3356A>T:p.Y1119F
chr7	91630394	G	C	44.4	SNV	---	AKAP9	NM_005751:exon8:c.1163G>C:p.R388T
chr8	118825130	G	A	54.8	SNV	COSM1454473	EXT1	NM_000127:exon8:c.1703C>T:p.T568M
chr8	42166476	G	A	38.5	SNV	COSM1099990	IKBKB	NM_001556:exon8:c.625G>A:p.G209S
chr17	7577106	G	A	100.0	SNV	COSM10939	TP53	NM_000546:exon8:c.832C>T:p.P278S
chr19	18856733	A	G	40.0	SNV	---	CRTC1	NM_015321:exon3:c.344A>G:p.H115R

Abbreviations: SNV, single nucleotide variant; INS, insertion; DEL, deletion.

[a]Only mutations in 409 cancer-related genes (see Table S4) were listed.

[b]Aberrant splicing was detected with Integrative Genomics Viewer.

Supplementary table 6: Summary of immunohistochemistry analysis for mismatch repair proteins in the primary tumor and spheroids in four hypermutated gastric cancer (GC) cases.

	MSH2				MSH6			
	Normal epithelium		Cancer		Normal epithelium		Cancer	
	Primary	Spheroids	Primary	Spheroids	Primary	Spheroids	Primary	Spheroids
HG3T	+	+	+	+	+	+	+	+
HG10T	+	+	+	+	+	+	+	+
HG13T	+	+	+	+	+	+	+	+
HG17T	+	+	+	+	+	+	+	+

	MLH1				PMS2			
	Normal epithelium		Cancer		Normal epithelium		Cancer	
	Primary	Spheroids	Primary	Spheroids	Primary	Spheroids	Primary	Spheroids
HG3T	+	+	–	–	+	+	–	–
HG10T	+	+	–	–	+	+	–	–
HG13T	+	+	–	–	+	+	–	–
HG17T	+	+	–	–	+	+	–	–

Abbreviations: +, positive; –, negative.